1-1-1983

Simulation and analysis of digital frequency modulation.

Arif Kareem

SIMULATION AND ANALYSIS OF DIGITAL FREQUENCY MODULATION

by

Arif Kareem

A Thesis

Presented to the Graduate Committee

of Lehigh University

in Candidacy for the Degree of

Master of Science

in

Electrical Engineering

Lehigh University

1980

This thesis is accepted and approved in partial fulfillment of the requirements for the degree of Master of Science

August 14, 1960
date

Professor in Charge

Chairman of the Department

ACKNOWLEDGEMENTS

I wish to express my deep gratitude to my thesis adviser, Professor Bruce D. Fritchman, for the guidance and the encouragement he gave me to undertake this project. I would also like to thank Professor Kalyan Mondal for his valuable suggestions. Finally, I wish to thank Mrs. Connie Weaver for typing the manuscript.

TABLE OF CONTENTS

LIST OF FIGURES

ABSTRACT

A numerical technique is developed in this thesis to find the spectrum of a frequency modulated signal and to recover the transmitted signal from this spectrum. Analysis of frequency shift keying is done using this algorithm. Results obtained using computer simulation, show that restricting the bandwidth of a frequency shift keyed system has significant effects on the transition time and mean-square-error of the received data pulse. Pulse shapes suitable for telemetry purpose are examined and an optimum pulse satisfying the telemetry standards has been designed. In addition, this technique is used to evaluate some work done by other researchers related to narrow band frequency shift keying.

CHAPTER 1

INTRODUCTION

This thesis develops an algorithm to find the spectrum of a frequency modulated signal for any modulating signal. Much research has been done in the area of frequency modulation, but computation of the exact spectrum for a general modulating signal is not possible. This work introduces a numerical technique to closely approximate the spectrum using a digital computer. A digital computation procedure is also developed to recover the modulating signal from the FM spectrum.

With the help of this work, investigation of the effects of restricted bandwidth on frequency shift keyed signals is possible. This research ellaborates on the related work done on frequency shift keying by Kotelnikov [2] and Salz [6], enabling the digital communication engineers to have a broader understanding of the time domain behaviour of this important digital data transmission system.

Chapter 2 gives a basic background about a frequency modulated signal. This is followed by the development of the algorithm to find the spectrum of an FM signal and the recovery of the transmitted signal from the spectrum thus obtained.

Chapter 3 introduces frequency shift keying with relationship to the work done by other researchers. Chapter 4 introduces an important problem and describes an approach to solving it. Work done related to the pulse shaping for telemetry purpose is also included in the same chapter. Chapter 5 summarizes the results of this investigation and conclusion drawn from it.

The flow chart of the computer program used for simulating the digital frequency modulated system is given in the appendix.

CHAPTER 2

FREQUENCY MODULATED SYSTEMS

2.0 Introduction

In this chapter the basic concepts concerning frequency modulated signals are reviewed. Analytic expressions are found and discussion about the spectrum is made. This is followed by the steps undertaken to develop an algorithm to find the spectrum of an FM signal and to recover the transmitted modulating signal from the spectrum.

2.1 Basic Background

Frequency modulation is a type of modulation in which the frequency of the carrier is varied in accordance with the amplitude of the modulating signal and the envelope of the resultant wave is held constant. Consider a constant amplitude sinusoid which can be represented by a phasor with magnitude A and a phase angle $\theta(t)$ as shown in Figure 2.1. If $\theta(t)$ increases linearly with time (that is $\theta(t) = \omega_c t$) it is said that the phasor has an angular velocity or 'frequency' of ω_c radians per second. If this frequency is not constant, it is still possible to write a relation between the instantaneous frequency $\omega_i(t)$ and $\theta(t)$

$$\omega_i(t) = d\theta/dt \qquad (2.1)$$

Integrating equation (2.1) gives

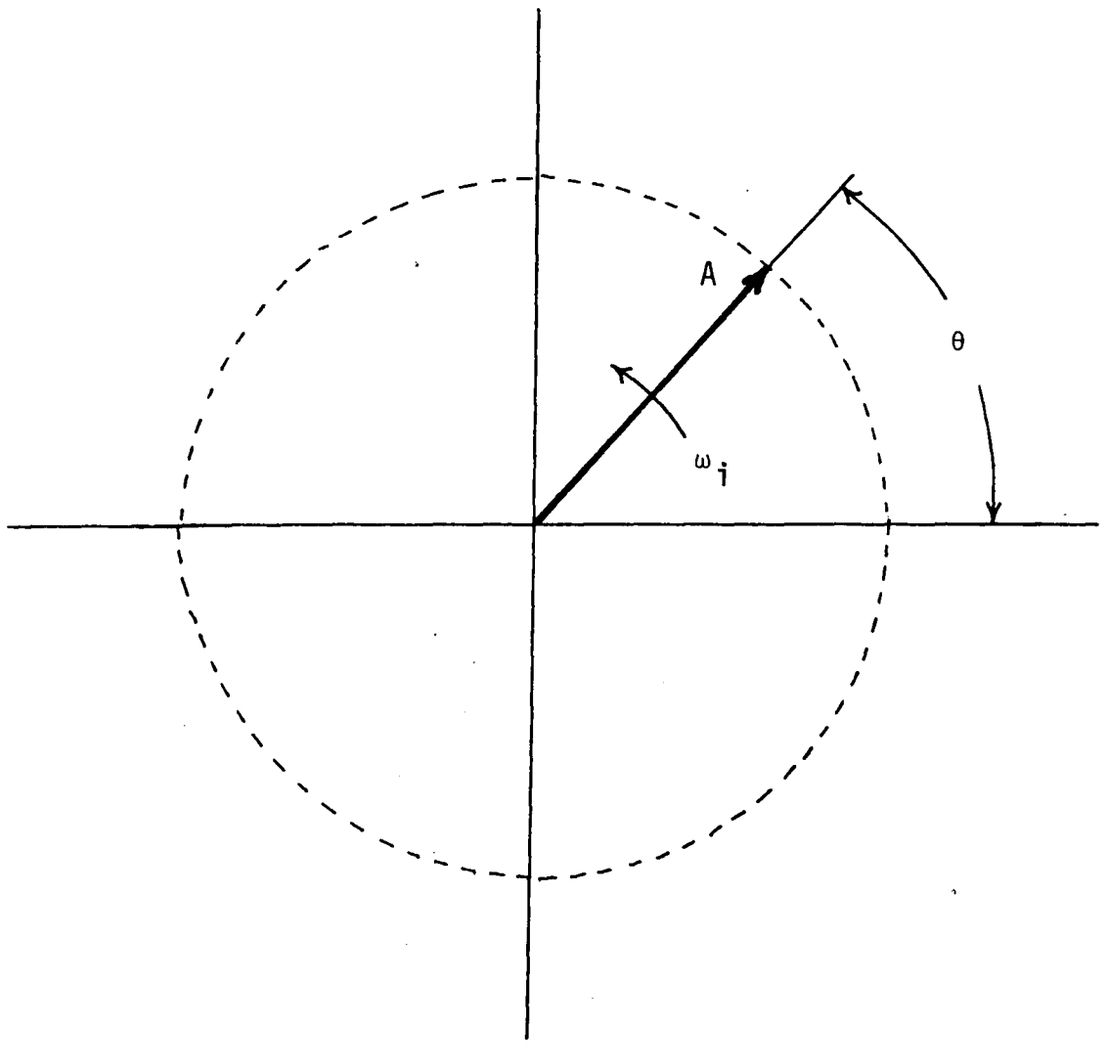

Fig. 2.1 - Phasor representation of a sinusoid

$$\theta(t) = \int_0^t \omega(\lambda)d\lambda \qquad (2.2)$$

Now if the instantaneous frequency is made proportional to the information (modulating signal), then

$$\omega_i = \omega_c + k_f f(t) \qquad (2.3)$$

where ω_c and k_f are constants which represent the carrier frequency and frequency deviation constant, respectively. Since the frequency is linearly proportional to f(t), this type of modulation, as noted before, is called Frequency Modulation. In general the modulated signal can be written as

$$\phi_{FM}(t) = A \cos(\omega_c t + k_f \int_0^t f(t)dt) \qquad (2.4)$$

$$= \mathrm{Re}[A \exp\{j(\omega_c t + k_f \int_0^t f(t)dt)\}] \qquad (2.5)$$

Figure 2.2 gives an example of a frequency modulated signal.

To lay the groundwork for the detailed analysis of an FM signal spectrum, the Fourier series expansion of an FM signal modulated by a single sinusoidal waveform is obtained. Let

$$f(t) = a \cos\omega_m t \qquad (2.6)$$

Now from equation (2.3)

$$\omega_i = \omega_c + k_f f(t)$$

$$= \omega_c + a\, k_f \cos\omega_m t \qquad (2.7)$$

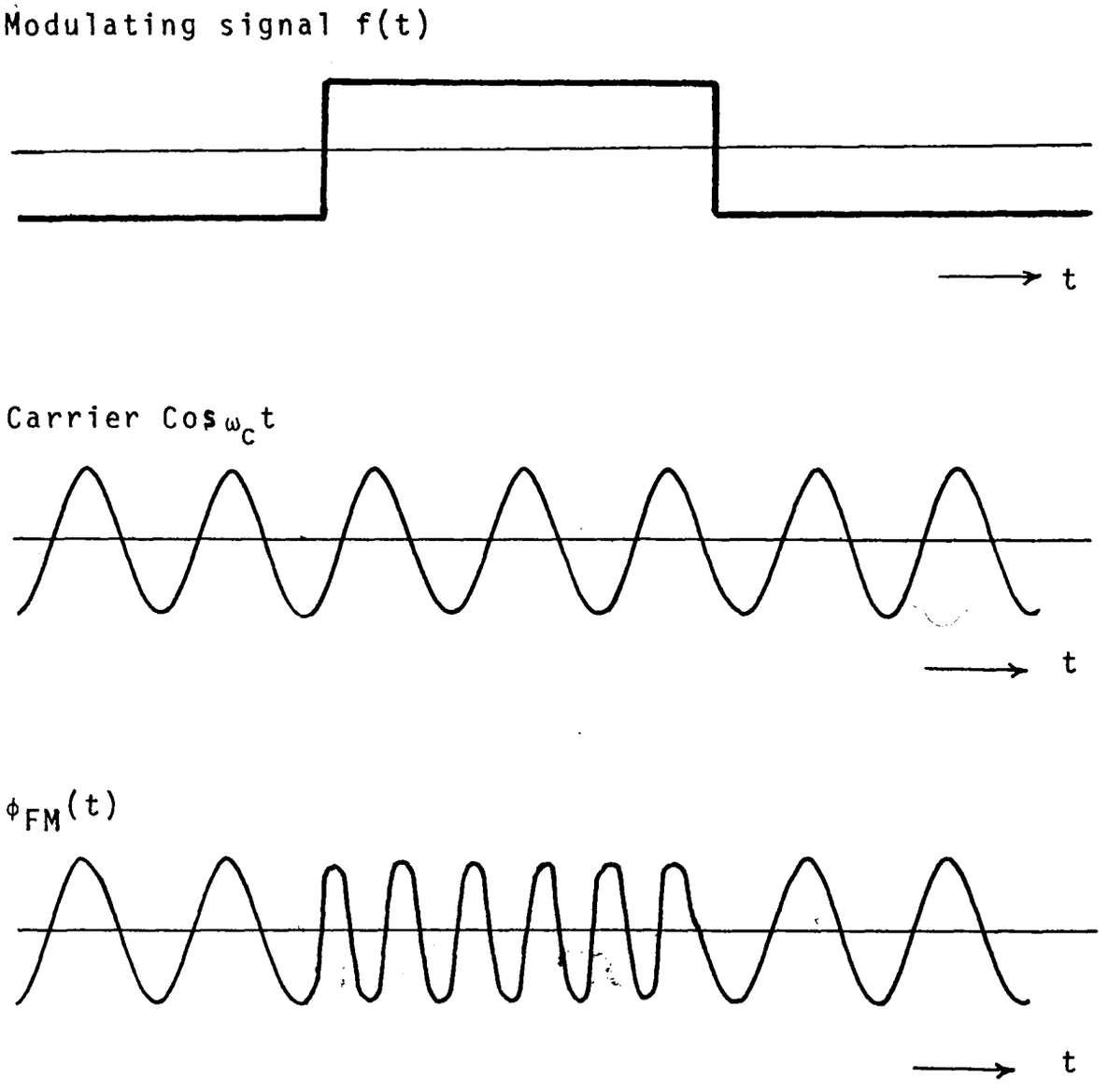

Fig. 2.2 - Frequency modulation waveforms

Defining a new constant $\Delta\omega = a\, k_f$, called the maximum frequency deviation, the instantaneous frequency, ω_i, is given by

$$\omega_i = \omega_c + \Delta\omega \, \mathrm{Cos}\omega_m t \tag{2.8}$$

The phase of this FM signal is

$$\begin{aligned}\theta(t) &= \omega_c t + \Delta\omega/\omega_m \, \mathrm{Sin}\omega_m t \\ &= \omega_c t + \beta \, \mathrm{Sin}\omega_m t \end{aligned} \tag{2.9}$$

where β is a dimensionless ratio called the modulation index. The resulting FM signal is

$$\phi_{FM}(t) = A \, \mathrm{Cos}(\omega_c t + \beta \, \mathrm{Sin}\omega_m t) \tag{2.10a}$$

$$= \mathrm{Re}[A \exp(j\omega_c t + j\beta \, \mathrm{Sin}\omega_m t)] \tag{2.10b}$$

The exponential in equation (2.10b) is a periodic function of time with fundamental frequency, ω_m rad/sec. The Fourier series for it can be expressed as

$$\exp(j\beta \, \mathrm{Sin}\omega_m t) = \sum_{n=-\infty}^{\infty} F(n) \exp(jn\omega_m t), \tag{2.11}$$

where

$$F(n) = \frac{1}{T} \int_{-T/2}^{T/2} \exp(j\beta \, \mathrm{Sin}\omega_m t) \exp(-jn\omega_m t) dt \tag{2.12}$$

This integral cannot be expressed in closed form and has been extensively tabulated as a function of 'n' and 'β' and is called the Bessel function [5] of the first kind. It is denoted $J_n(\beta)$ and is said to be of order 'n' and argument 'β'. Hence equation (2.10) can be expressed as

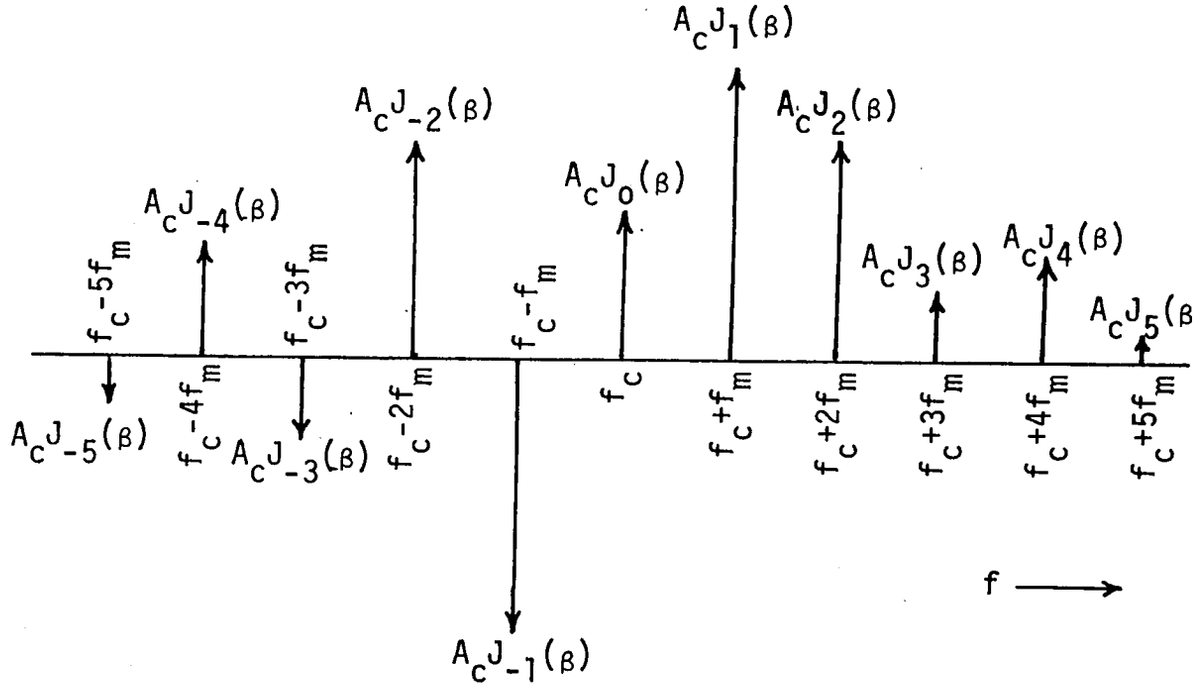

Fig. 2.3 - Positive frequency FM spectrum

$$\phi_{FM}(t) = \mathrm{Re}[A \exp(j\omega_c t) \sum_{n=-\infty}^{\infty} J_n(\beta) \exp(jn\omega_m t)] \quad (2.13)$$

$$= A \sum_{n=-\infty}^{\infty} J_n(\beta) \cos(\omega_c + n\omega_m)t \quad (2.14)$$

This result makes it clear that the FM signal has a theoretically infinite number of sidebands and hence infinite bandwidth. However, the magnitude of the spectral components of higher order sidebands become negligible; and for all practical purposes the power is contained within a finite bandwidth. Carson [5] has given an approximate formula for the bandwidth of an FM signal as

$$BW = 2(D+1)W \ , \quad (2.15)$$

where, D, is the ratio of the maximum frequency deviation to the bandwidth (W) of the modulating signal f(t). Figure 2.3 shows the positive frequency spectrum of a frequency modulated signal.

2.2 Algorithm Development

As may be seen from equation (2.4), an FM signal may be expressed as

$$\phi_{FM}(t) = A \cos(\omega_c t + k_f \int_0^t f(t)dt)$$

In order to find an expression for any arbitrary signal f(t), it is first necessary to evaluate the integral in the argument of the cosine. This may be done by expressing f(t) in terms of its trigonometric Fourier series

provided it is a periodic signal. Such a restriction still retains the generality of the analysis to a great extent. Equation (2.4) then becomes

$$\phi_{FM}(t) = A\,\mathrm{Cos}\Big[\omega_c t + k_f \int_0^t (a_1\mathrm{Cos}\omega_1 t + a_2\mathrm{Cos}\omega_2 t + \text{----} + b_1\mathrm{Sin}\omega_1 t + b_2\mathrm{Sin}\omega_2 t + \text{----})dt \qquad (2.16)$$

This may be recognized as an expression for multitone frequency modulation. If V is the amplitude of f(t), then $f_n(t) = f(t)/V$ is called normalized f(t). The expression for an FM signal can then be written as

$$\begin{aligned}\phi_{FM}(t) &= A\,\mathrm{Cos}(\omega_c t + V\,k_f \int f_n(t)dt)\\ &= A\,\mathrm{Cos}(\omega_c t + \beta_1\mathrm{Sin}\omega_1 t + \beta_2\mathrm{Sin}\omega_2 t + \text{----}\\ &\quad -\alpha_1\mathrm{Cos}\omega_1 t - \alpha_2\mathrm{Cos}\omega_2 t\text{----})\\ &= \mathrm{Re}[A\,\exp(j\omega_c t)\{\exp(j\beta_1\mathrm{Sin}\omega_1 t)\\ &\quad \exp(j\beta_2\mathrm{Sin}\omega_2 t)\text{----}\}\{\exp(-j\alpha_1\mathrm{Cos}\omega_1 t)\\ &\quad \exp(-j\alpha_2\mathrm{Cos}\omega_2 t)\text{----}\}]\end{aligned}$$

Each exponential term in the above equation may be expressed in terms of Bessel functions, i.e.,

$$\begin{aligned}\phi_{FM}(t) = \mathrm{Re}[A\,\exp(j\omega_c t)\{&\sum_{n_1=-\infty}^{\infty} J_{n_1}(\beta_1)\\ &\exp(jn_1\omega_1 t)\sum_{n_2=-\infty}^{\infty} J_{n_2}(\beta_2)\exp(jn_2\omega_2 t)\text{----}\}\\ &\{\sum_{k_1=-\infty}^{\infty} S_{k_1}(\alpha_1)\exp(jk_1\omega_1 t)\sum_{k_2=-\infty}^{\infty} S_{k_2}(\alpha_2)\\ &\exp(jk_2\omega_2 t)\text{----}\}] \qquad (2.17)\end{aligned}$$

where

$$\sum_{\ell=-\infty}^{\infty} S_\ell(x) = \sum_{\ell=-\infty}^{\infty} (j)^{-\ell} J_\ell(x) \qquad (2.18)$$

equation (2.18) may further be expressed as

$$\phi_{FM}(t) = A[\sum_{n_1}\sum_{n_2}\text{----}\sum_{n_m}\sum_{k_1}\sum_{k_2}\text{----}\sum_{k_m}\{J_{n_1}(\beta_1)J_{n_2}(\beta_2)\text{----}$$
$$J_{n_m}(\beta_m)S_{k_1}(\alpha_1)S_{k_2}(\alpha_2)\text{----}S_{k_m}(\alpha_m)\}\text{Cos}(\omega_c +$$
$$n_1\omega_1 + n_2\omega_2 + \text{----}n_m\omega_m + k_1\omega_1 + k_2\omega_2$$
$$+ \text{----}k_m\omega_m)t] \qquad (2.19)$$

It is clear that the spectrum of an FM signal contains single sideband terms ($\omega_c \pm n_1\omega_1$ or $k_1\omega_1$), ($\omega_c \pm n_2\omega_2$ or $k_2\omega_2$),----($\omega_c \pm n_m\omega_m$ or $k_m\omega_m$), corresponding to the frequencies ω_1, ω_2----ω_m. In addition there are cross modulation terms ($\omega_c \pm n_1\omega_1 \pm n_2\omega_2 \pm$----$n_m\omega_m \pm k_1\omega_1 \pm k_2\omega_2$----$k_m\omega_m$).

In the algorithm developed in this study to determine the spectrum of an FM signal, eight cosine terms, eight sine terms, or four each of cosine and sine terms of the Fourier series approximating the modulating signal, f(t), are accommodated. First the modulation indices are calculated from the given data regarding the amplitude of the modulating signal, f(t), the maximum frequency deviation and the Fourier coefficients of f(t). Then the Bessel coefficients [$J_n(x)$, $S_k(x)$] are evaluated up to an order beyond which their magnitude becomes almost negligible.

Since there could be different combinations of 'n' and 'k' that may yield spectral terms of the same frequency, care was taken to collect all such terms and arrange the sidebands in increasing order. Knowing that the total power in an FM signal is $A^2/2$, the power in the spectral terms outside the frequency band considered, can also be calculated.

CHAPTER 3

APPLICATION TO FREQUENCY SHIFT KEYING

3.0 Introduction

This chapter deals with data transmission using frequency modulation. A further description of frequency shift keying is given. Later in the chapter other work is discussed, with emphasis on problems not previously considered. Application of the simulation program, described in Chapter 2, to the analysis of frequency shift keying is also discussed.

3.1 Frequency Shift Keying

The most commonly used digital communication systems for radio frequency transmission of binary information are frequency shift keying (FSK) and phase shift keying (PSK). In the case of binary FSK, two oscillators operating at different frequencies may be used to transmit the binary information. Alternatively, one variable frequency oscillator may be used. When a binary 0 (zero) is to be transmitted, a burst of $\text{Cos}\omega_0 t$ is generated and when a binary 1 (one) is to be transmitted a burst of $\text{Cos}\omega_1 t$ is generated as shown in Figure 3.1. This can be seen to be a form of frequency modulation where the modulating signal is always one of two possible values. Since only two frequencies are used, the modems need not be as sophisticated

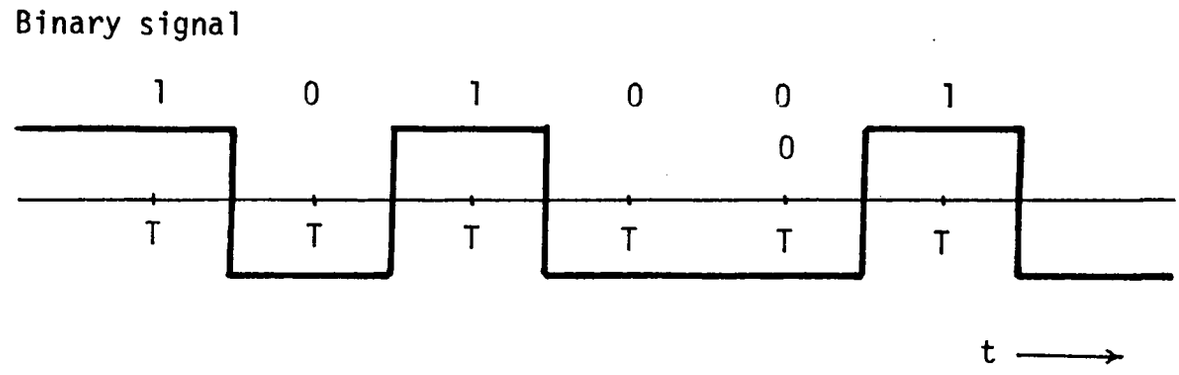

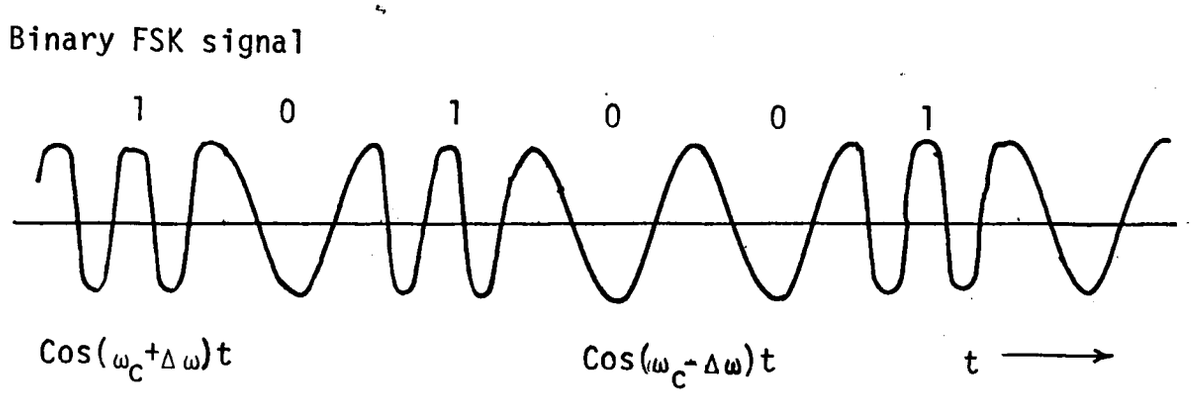

Fig. 3.1 - Binary frequency shift keying waveforms

as they are for a general FM system. As might be intuitively seen, the farther the separation between the two frequencies the easier it would be to distinguish between them, even in the presence of some background noise. However, a wider separation of the frequencies implies a larger frequency deviation, which according to equation (2.15), increases the bandwidth of the FM signal. Thus a trade-off between the bandwidth and noise immunity is required in the design of an FSK system.

From Figure 3.2 an expression for the phase angle of an FM signal modulated by a square wave may be written as

$$\theta(t) = \omega_c t + \Delta\omega \int_0^t f(\lambda)d\lambda$$

$$= \omega_c t + \phi(t)$$

$$\phi(t) = \Delta\omega t \qquad -T/4 \leq t \leq T/4 \qquad (3.1a)$$

$$= \Delta\omega(T/2 - t) \qquad T/4 \leq t \leq 3T/4 \qquad (3.1b)$$

Since $\phi(t)$ is periodic with a period T, so it can be expressed by Fourier series

$$\exp(j\phi(t)) = \sum_{n=-\infty}^{\infty} F_n \exp(jn\omega_o t)$$

$$F_n = \frac{1}{T}\int_0^T \phi(t)\exp(-jn\omega_o t)dt$$

$$= \frac{1}{2}[Sa\{\frac{\pi}{2}(z-n)\} + (-1)^n Sa\{\frac{\pi}{2}(z+n)\}] \qquad (3.2)$$

where

$$z = \Delta\omega/\omega_o$$

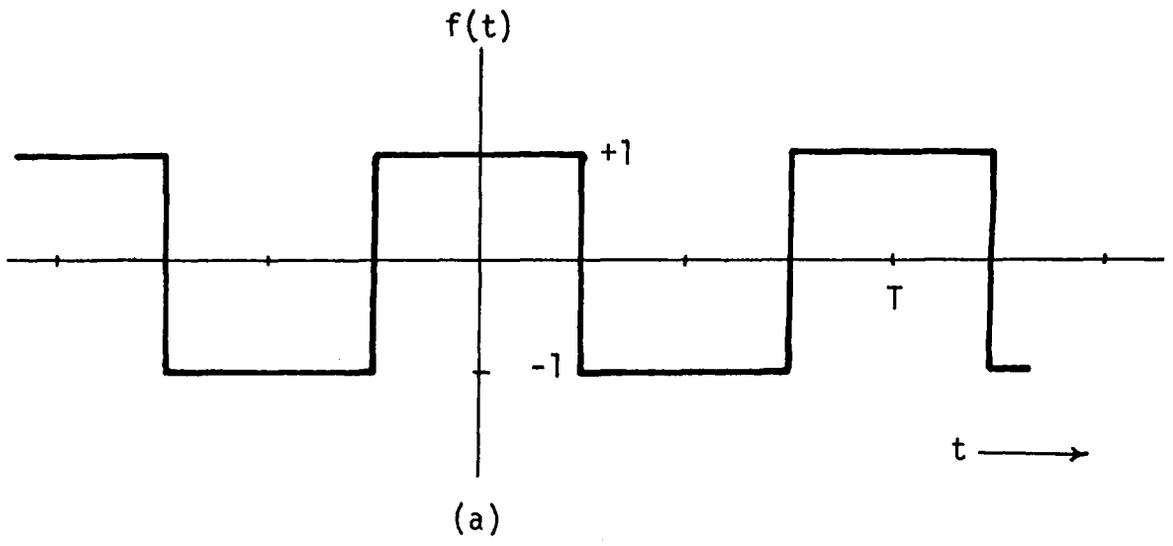

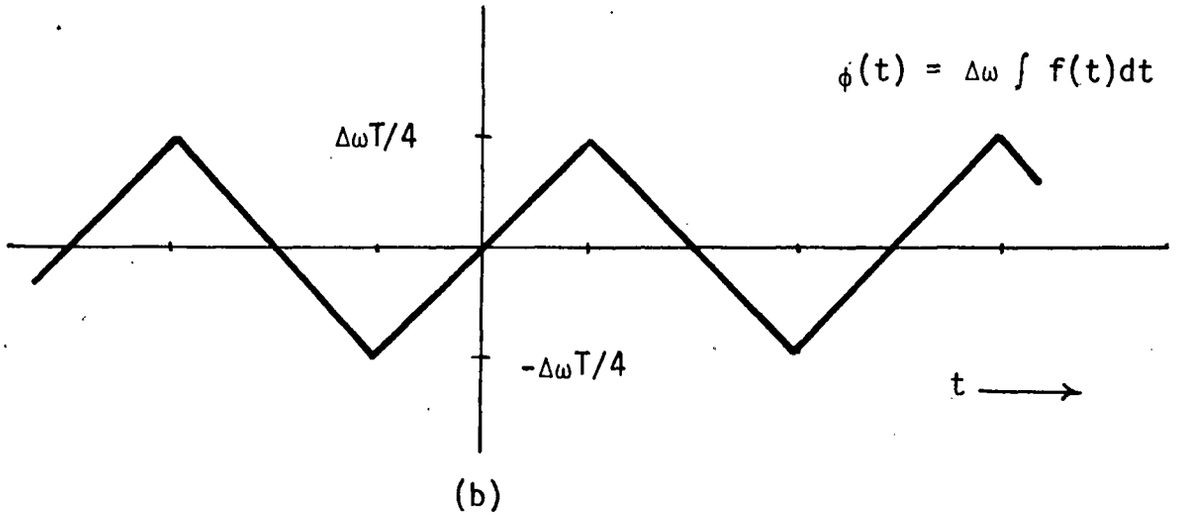

Fig. 3.2 - Periodic binary frequency shift keying

The analytic expression for an FM signal is

$$\phi_{FM}(t) = \mathrm{Re}[A \exp(j\omega_c t) \exp(j\phi(t))]$$

$$= A \sum_{n=-\infty}^{\infty} F_n \mathrm{Cos}(\omega_c t + n\omega_o t) \qquad (3.3)$$

The Fourier series representation of a periodic FSK signal is given by equation (3.2) and equation (3.3).

Under certain circumstances it is possible to increase transmission efficiency by using multi-level frequency shift keying. Given a source which produces k different symbols, or a binary source in which m symbols have been grouped to produce $k = 2^m$ sequences, a voltage level can be associated with each of the possible symbols as shown in Figure 3.3. Each symbol will represent $\log_2 k$ bits of information and for the same data rate as for the binary transmission, only $1/\log_2 k$ times as many pulses per second are transmitted, thus improving the transmission efficiency. The baseband signal which can now be used to modulate a carrier becomes

$$f(t) = \sum_k a_k \, x(t-kT) \qquad (3.4)$$

where x(t) is any arbitrary pulse of unit height with a duration of T seconds and a_k is the data sequence. The modulated signal will be transmitted via a channel and at the receiving end different demodulation schemes may be employed to recover the modulating signal. An estimate

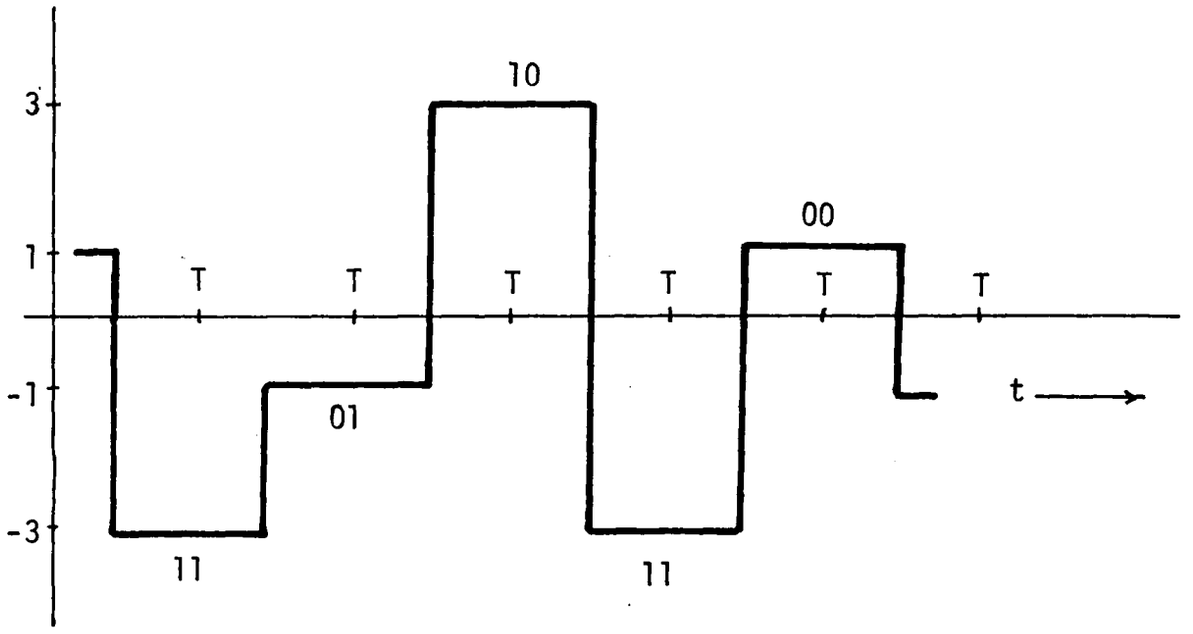

Multi-level digital FM wave

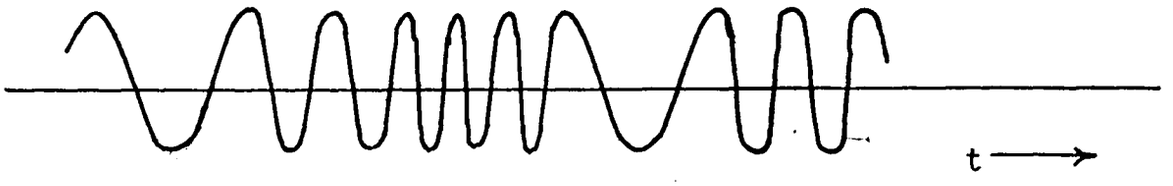

Fig. 3.3 - Multilevel frequency shift keying waveforms

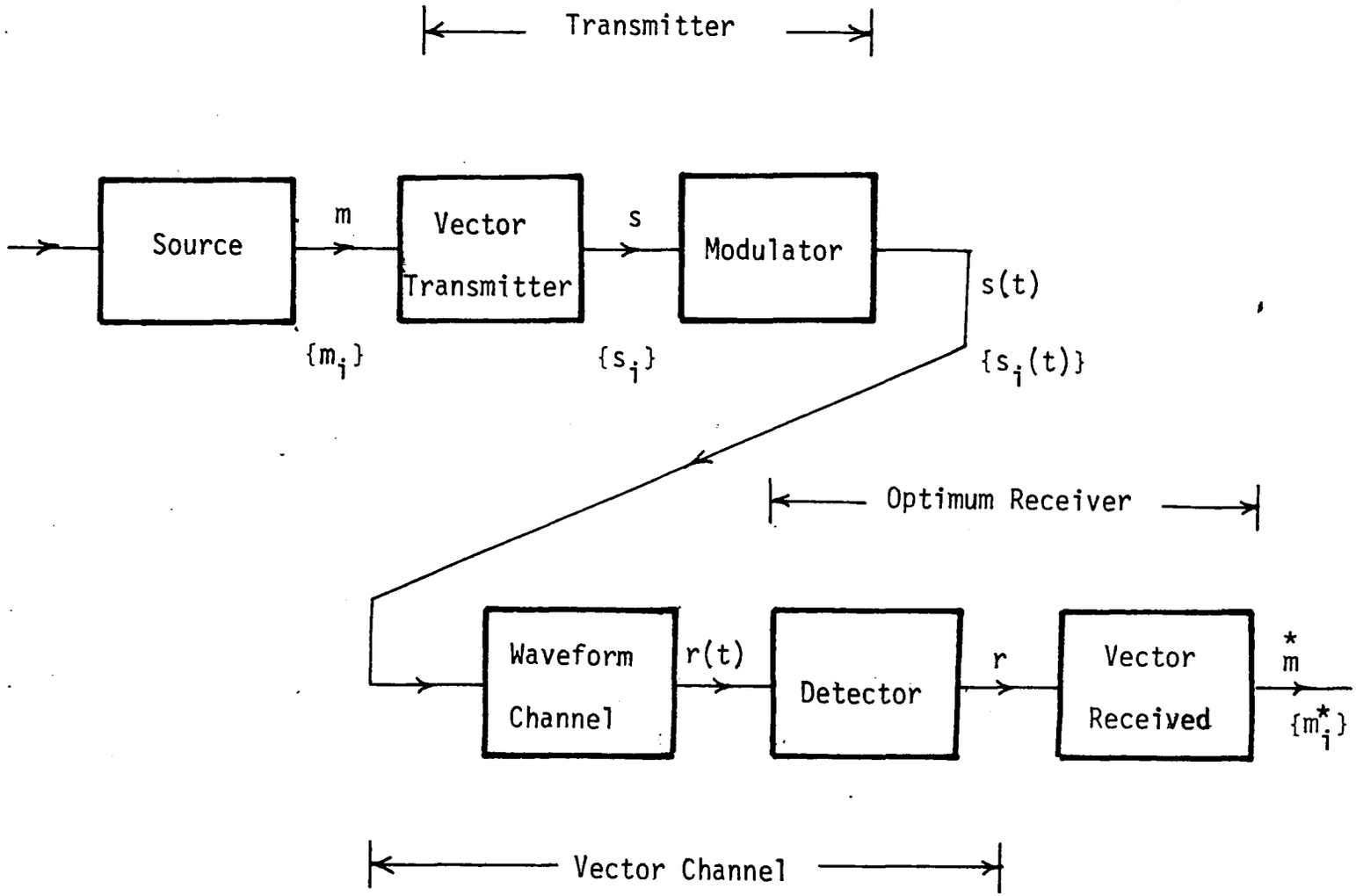

Fig. 3.4 - Vector form of representing a data system

of the transmitted data can then be determined from the demodulated signal.

3.2 Kotelnikov's Analysis

Kotelnikov [2] has analyzed binary FSK in detail and has suggested some design procedures to obtain an optimum system with respect to noise immunity. He represented the FSK system in the vector form as shown in Figure 3.4, where $\{m_i\}$ is the set of symbols to be transmitted, $\{S_i(t)\}$ is the set of waveforms representing these symbols, $\{r_i(t)\}$ is the set of received waveforms and $\{m_i^*\}$ is the set of received symbols. Kotelnikov showed that the optimum receiver sets m^* equal to m_k if the decision function

$$M_{in_i}[|r-S_i|^2 - N_o \ell n\ P(m_i)] \quad i = 1,2,---M \tag{3.5}$$

is minimum for $i = k$, where $N_o/2$ is the power density spectrum of the additive white Gaussian noise and $P(m_i)$ is the apriori probability of the transmitted symbol. The boundary of the decision region for antipodal signals may be obtained by solving

$$|r-S_1|^2 - N_o \ell n\ P(m_1) = |r-S_o|^2 - N_o \ell n\ P(m_o) \tag{3.6}$$

where $r = (r_1, r_2)$ as shown in Figure 3.5a. For any value of r_2 the equation (3.6) becomes

$$|r_1 + d/2|^2 - N_o \ell n\ P(m_1) = |r_1 - d/2|^2 - N_o \ell n\ P(m_o) \tag{3.7}$$

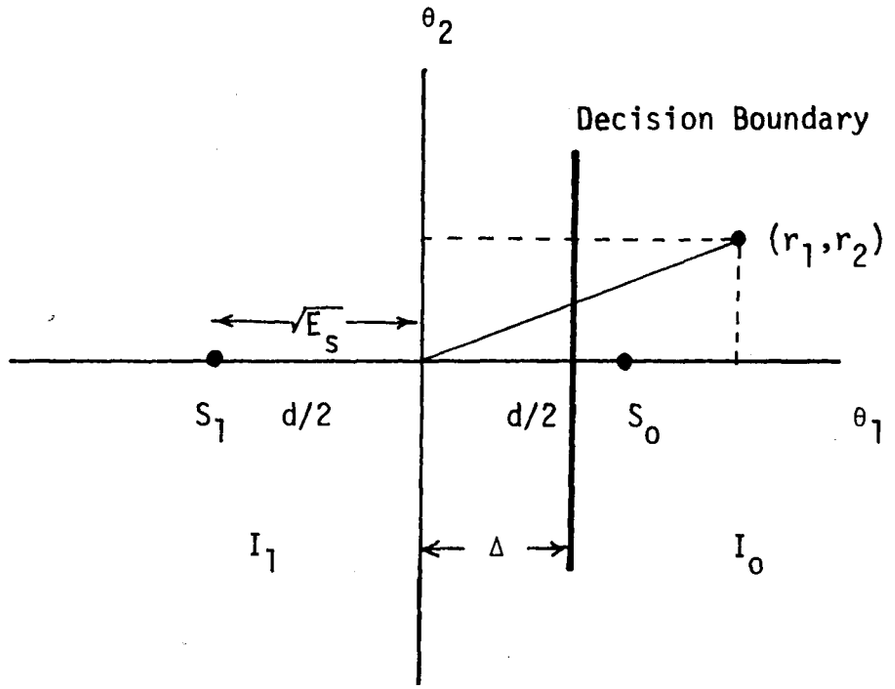

Fig. 3.5(a) - Decision regions of an antipodal signal with unequal probabilities

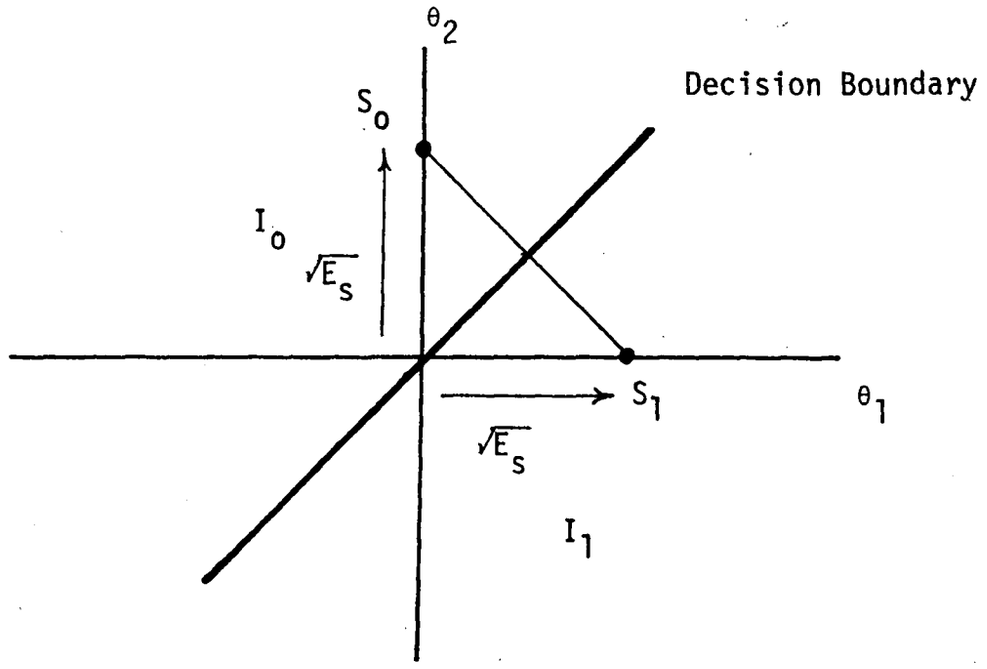

Fig. 3.5(b) - Decision regions of an orthogonal signal

Let Δ be the value of r_1 satisfying equation (3.7), then

$$\Delta = N_0/2d \ \ell n \ P(m_1)/P(m_0) \qquad (3.8)$$

Depending upon the ratio $P(m_1)/P(m_0)$, the decision region will shift accordingly in the direction of either S_1 or S_0.

The probability of error, P(E), of binary FSK is given by

$$P(E) = P(m_1) \ P(E|m_1) + P(m_0) \ P(E|m_0) \qquad (3.9)$$

where

$$P(E|m_1) = P(n \geq d/2 + \Delta)$$

$$P(E|m_0) = P(n \leq -(d/2 - \Delta))$$

are called the aposteriori probabilities of the transmitted symbols and 'n' is the additive Gaussian noise with zero mean. Now the aposteriori probabilities can be expressed in terms of the complementary error function, Q(x), and equation (3.9) becomes

$$P(E) = P(m_1) \ Q(\alpha_{12}) + P(m_0) \ Q(\alpha_{21}) \qquad (3.10)$$

where

$$\alpha_{12} = d + 2\Delta/\sqrt{2} \ N_0 \text{ and } \alpha_{21} = d - 2\Delta/\sqrt{2} \ N_0$$

Consequently, P(E) will be small if the argument of Q(x) is large. Since $\Delta = N_0/2d \ \ell n \ P(m_1)/P(m_0)$ from equation (3.8),

$$\alpha_{12} = \alpha - 1/2\alpha \ \ell n \ P(m_1)/P(m_0) \qquad (3.11a)$$

$$\alpha_{21} = \alpha + 1/2\alpha \ \ell n \ P(m_1)/P(m_0) \qquad (3.11b)$$

where

$$\alpha = d/\sqrt{2}\ N_0$$

and

$$d^2 = \int_{-\infty}^{\infty} [S_0(t) - S_1(t)]^2 dt \qquad (3.12)$$

Kotelnikov argued that the probability of error which determines the noise immunity depends upon two factors — the ratio $P(m_1)/P(m_0)$ and $\alpha = d/\sqrt{2}\ N_0$. The first factor depends only on the transmitted message and the second factor depends on the ratio of the energy of the difference signal to the mean-square-value of the noise. The larger the ratio the smaller the probability of error. For a given noise power density, only the energy of the difference signal can be changed to achieve a required noise immunity. Obviously, systems for which this energy is the largest afford the best noise immunity with the condition that the receivers are appropriately designed.

In geometric terms, α and hence noise immunity are determined by the distance between the points representing the received and the transmitted signal in the signal space as shown in Figure 3.5. The noise immunity achieved may therefore be made large by increasing this distance. Some design parameters were also suggested by Kotelnikov which may be viewed by further analysis of the quantity $\alpha = d/\sqrt{2}\ N_0$

$$\alpha^2 = \frac{1}{2N_o} \int_{-\infty}^{\infty} [S_o(t) - S_1(t)]^2 dt \qquad (3.13)$$

For the present analysis

$$S_o(t) = A \cos\omega_1 t \qquad o \leq t \leq T \qquad (3.14)$$

$$S_1(t) = A \cos\omega_2 t \qquad (3.15)$$

Thus, α^2 can be expressed as

$$\alpha^2 = \frac{A^2}{2N_o}[T - \frac{1}{\omega_1 - \omega_2}\{\sin(\omega_1 - \omega_2 T\}] \qquad (3.16)$$

Since the signal energy is given by

$$E_s = \int_{-T/2}^{T/2} f^2(t) dt \qquad (3.17)$$

or

$$E_s = \frac{A^2 T}{2}, \qquad (3.18)$$

equation (3.17) becomes

$$\alpha^2 = \frac{E_s}{N_o}[1 - \frac{\sin(\omega_1 - \omega_2)T}{(\omega_1 - \omega_2)T}] \qquad (3.19)$$

Equation (3.19) may be solved for $\omega_1 - \omega_2$

$$\frac{\omega_1 - \omega_2}{2\pi} = 2\Delta f = \frac{0.715}{T} \qquad (3.20)$$

Thus, for optimum noise immunity the difference between the two frequencies, which is known as peak to peak frequency deviation and is twice the frequency deviation, should be 0.715 of the bit rate. Kotelnikov's analysis assumes that all the sidebands of the FM wave are present and there is no filtering.

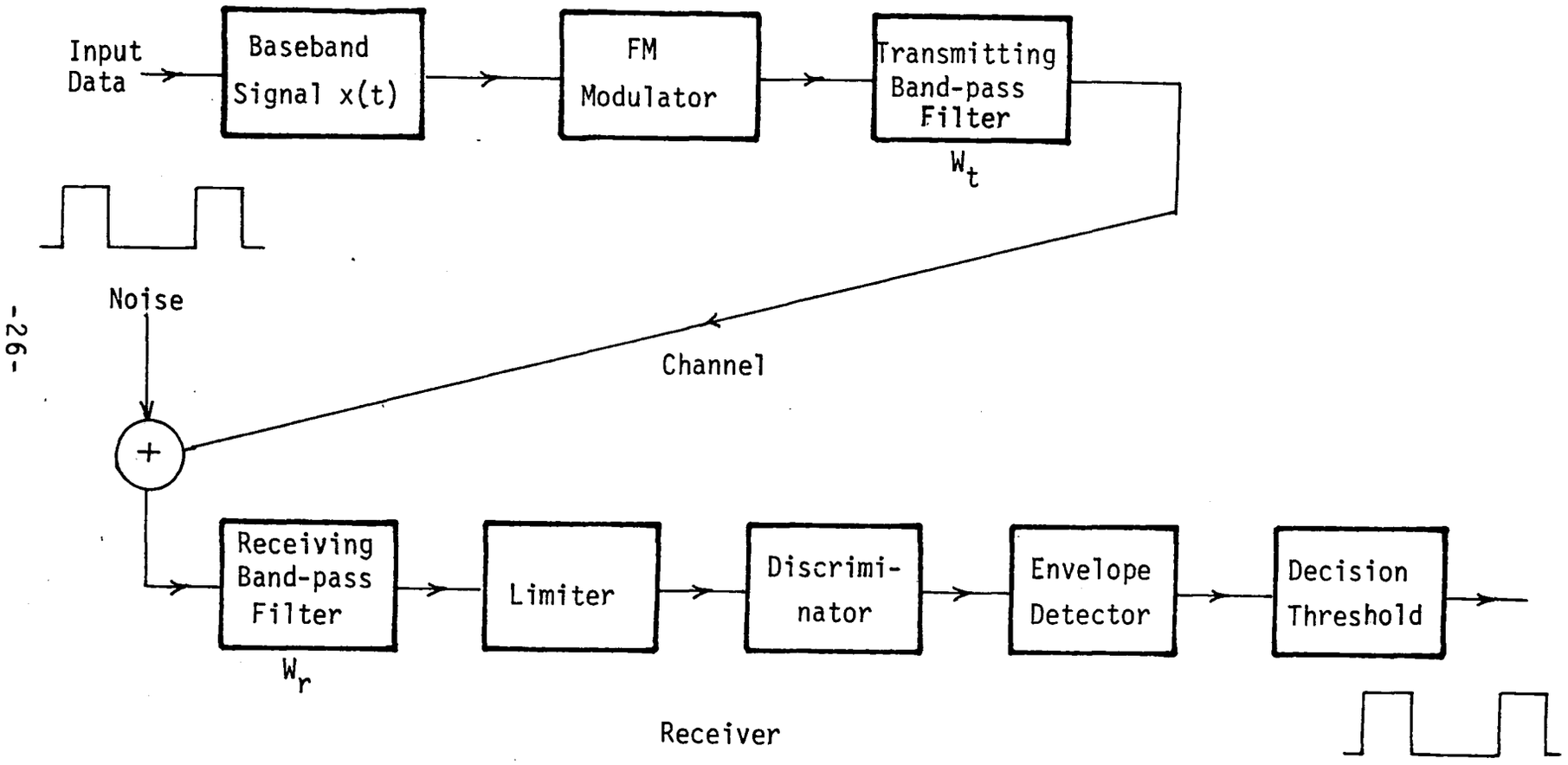

Fig. 3.6 - Digital FM data transmission system

3.3 Narrow Band Digital FM

After Kotelnikov's analysis of frequency shift keying, much work was done by other researchers particularly Salz [4] to find an optimum system employing lesser bandwidth. In his work Salz assumes a baseband signal having L possible, equally likely levels which are chosen as

$$a_n = 2K - (L+1) \tag{3.21}$$

where K = 1,2,----L for all n, and L is assumed even. He then suggests that for a frequency deviation,

$$\Delta\omega = \pi/LT \text{ or } \Delta f = 1/2LT, \tag{3.22}$$

inversely proportional to the bit rate and the number of levels, that most of the spectrum will be confined to a relatively narrow band. With some choice of frequency deviation and bit rate, if $\Delta\omega T/\pi$ equals unity, the spectrum spreads and most of the power tends to concentrate about the transmitted frequencies. The overall block diagram of the frequency shift keying system given by Salz is shown in Figure 3.6. In this system, filters have been added at both the transmitter and the receiver, with overall flat characteristic in the range of frequency in which the spectral components of the FM signal have the greatest strength, such that

$$W_r(\omega)\, W_t(\omega) = 1, \text{ for } \omega_c - 3\pi/2T \leq \omega \leq \omega_c + 3\pi/2T$$

where $W_r(\omega)$ and $W_t(\omega)$ are the receiver and the transmitter filter characteristics, respectively.

For binary transmission, this system has a peak-to-peak frequency deviation equal to 50 percent of the bit rate and a lesser spread of the significant sidebands because of the added filters as compared to Kotelnikov's optimum system employing a peak-to-peak frequency deviation of 71 percent of the bit rate. Despite the reduced bandwidth and the distortion caused by the filters, this system performs almost as well as other optimum systems like the commonly used differentially-coherent, phase modulation, but it enjoys the added advantage of simple instrumentation. However, reduction in the bandwidth may have effects on the received data pulse in the time domain. This problem, which has been ignored by Salz, is discussed in Chapter 4.

CHAPTER 4

SIMULATION AND ANALYSIS

4.0 Introduction

In this chapter an alogrithm for the demodulation of a digital frequency modulated system is discussed. This is followed by the application of different algorithms developed in this research to the problem of signal shaping for the purpose of telemetry. Later in the chapter, analysis of the simulation is given.

4.1 Demodulation Algorithm

In this study an algorithm was developed to recover the modulating signal from a frequency modulated signal based on the most commonly used demodulation scheme employing a limiter followed by a discriminator. The presence of the limiter is essential to obtain from the fluctuating amplitude FM signal (caused by simultaneous amplitude modulation) a constant-envelope FM signal. The differentiator output is another variable frequency sinusoid with an envelope containing the modulating signal which may be recovered by passing the output signal through an envelope detector. Once the modulating signal has been recovered, a decision about the transmitted data can be made. Figure 4.1 gives the block diagram of the demodulation scheme.

The Fourier series representation of the FM signal

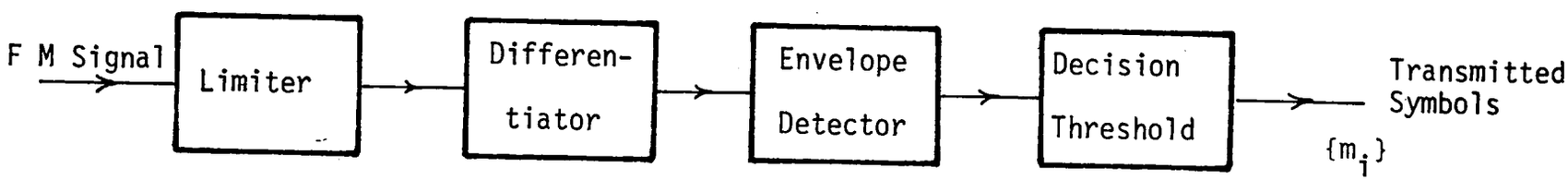

Fig. 4.1 - Block diagram of a limiter-discriminator detection system

described by equation (2.4) is

$$\phi_{FM}(t) = A\,\mathrm{Cos}(\omega_c t + k_f \int f(t)dt)$$
$$= c(0)\mathrm{Cos}\omega_c t + c(1)\mathrm{Cos}(\omega_c + \omega_m)t$$
$$+ c(-1)\mathrm{Cos}(\omega_c - \omega_m)t + c(2)\mathrm{Cos}(\omega_c + 2\omega_m)t$$
$$+ c(-2)\mathrm{Cos}(\omega_c - 2\omega_m)t + \text{----} \qquad (4.1)$$

To facilitate computer simulation the carrier term may be eliminated, then the resulting FM signal can be expressed as

$$\phi^*_{FM}(t) = A\,\mathrm{Cos}(k_f \int f(t)dt)$$
$$\simeq c(0) + [c(1)+c(-1)]\mathrm{Cos}\omega_m t$$
$$+ [c(2)+c(-2)]\mathrm{Cos}2\omega_m t + \text{----} \qquad (4.2)$$

Let

$$x(t) = c(0) + [c(1)+c(-1)]\mathrm{Cos}\omega_m t$$
$$+ [c(2)+c(-2)]\mathrm{Cos}2\omega_m t + \text{----} \qquad (4.3a)$$

$$\phi_{FM}(t) = A\,\mathrm{Cos}(k_f \int f(t)dt) \simeq x(t) \qquad (4.3b)$$

For a constant envelope FM signal, x(t) as given by equation (4.3a) should vary between A and -A. But x(t) is a trigonometric series approximating $\phi^*_{FM}(t)$, it may have a peak value A^*, not equal to A. In order to get a constant envelope FM signal, x(t) may be normalized to have a maximum value of A by multiplying with A/A^*. This operation is equivalent to using a limiter. The presence of the limiter is essential to obtain a true FM

signal before demodulation, so that the demodulated signal is a good replica of the modulating signal. After the limiter has been included, equation (4.3b) becomes

$$\phi^{*}_{FM}(t) = A \, \mathrm{Cos}(k_f \int f(t)dt) = A/A^{*} \; x(t) \qquad (4.4)$$

Differentiation of both sides of equation (4.4) gives

$$k_f \; f(t) \; \mathrm{Sin}(k_f \int f(t)dt) = -\frac{1}{A^{*}} \; \frac{dx(t)}{dt} = z(t)$$

$$k_f \; f(t) \; (\pm\sqrt{1-x^2(t)}) = z(t)$$

$$f(t) = \pm \, 1/k_f \; \frac{z(t)}{\sqrt{1-x^2(t)}} \qquad (4.5)$$

An algorithm for computer simulation may be written to recover the modulating signal from equation (4.5). Since $\mathrm{Cos}(\theta)$ is a periodic function with a period of 2π, many arguments of the cosine term in equation (4.4) give the same value of $\phi^{*}_{FM}(t)$. By selecting the constant, k_f, and the amplitude of the modulating signal low enough, the argument of the cosine term in equation (4.4) can be made to vary between $+\pi$ and $-\pi$. Obviously, minus sign may be chosen if the argument lies between $-\pi$ and 0 (zero).

4.2 Signal Shaping for Telemetry

In true FSK modulation, switching between frequencies occurs instantaneously which causes a broad spectrum. Therefore, in most narrowband systems, the FSK signal is filtered to meet spectral transmission requirements. Examination of the filtered FSK signal shows that the

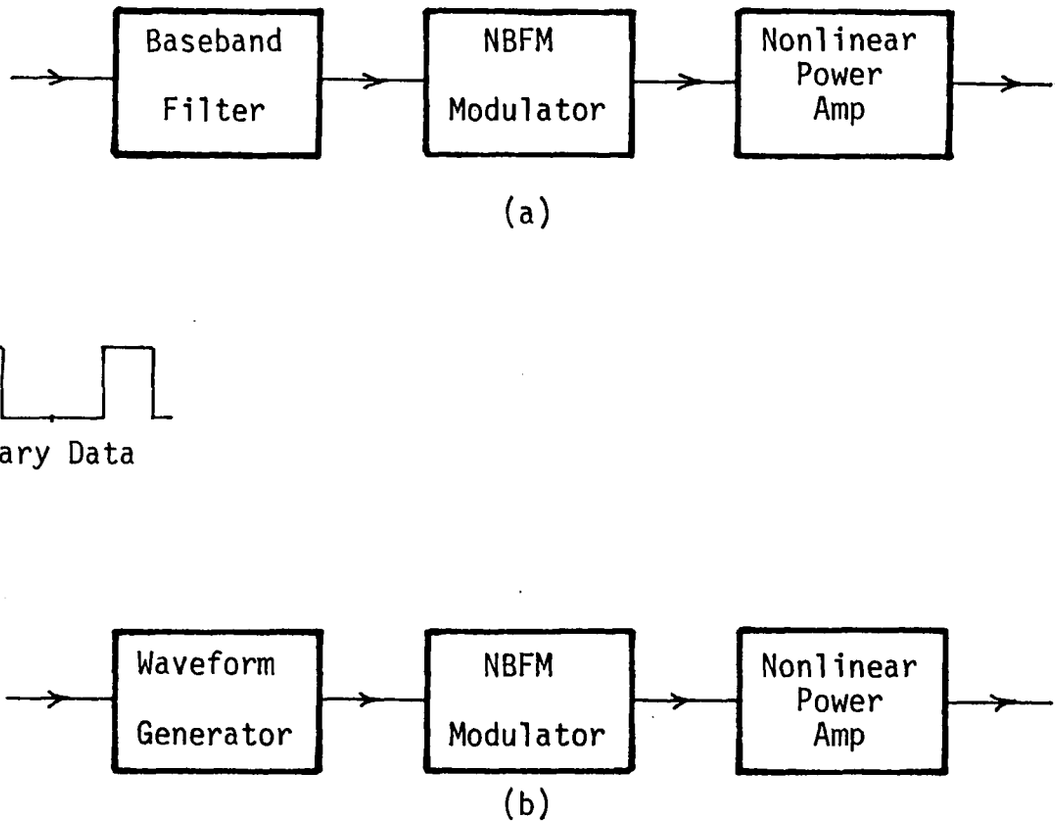

Fig. 4.2 - Band limiting an FM signal

frequency transitions are no longer instantaneous, but make smooth transitions. It is, therefore, the form of the transition which determines the shape of the modulated spectrum. This suggests an alternate method of band-limiting the FSK spectrum by appropriately shaping the modulating signal, which might be done directly by generating an appropriately shaped signal or by pre-filtering the data generated pulse train. Both methods are illustrated in Figure 4.2.

Special shaping by directly generating an appropriate modulating signal, as shown in Figure 4.2b, is the method now investigated. Determination of a modulating signal having "good" characteristics is accomplished by a combination of analysis, intuition and computer evaluation. One basic approach to limit the bandwidth of the FM signal is to limit the bandwidth of the modulating signal. In principle, if the receiver filters are matched to the modulated signal, the shape of the modulating signal is unimportant. But in practice, when limiters and other than matched filtering is used, the shape of the modulating signal is important. In general, the closer the modulating signal approaches the signal to which the receiver filters have been matched, the better the performance. From this point of view, since existing receivers are designed to handle filtered FSK signals,

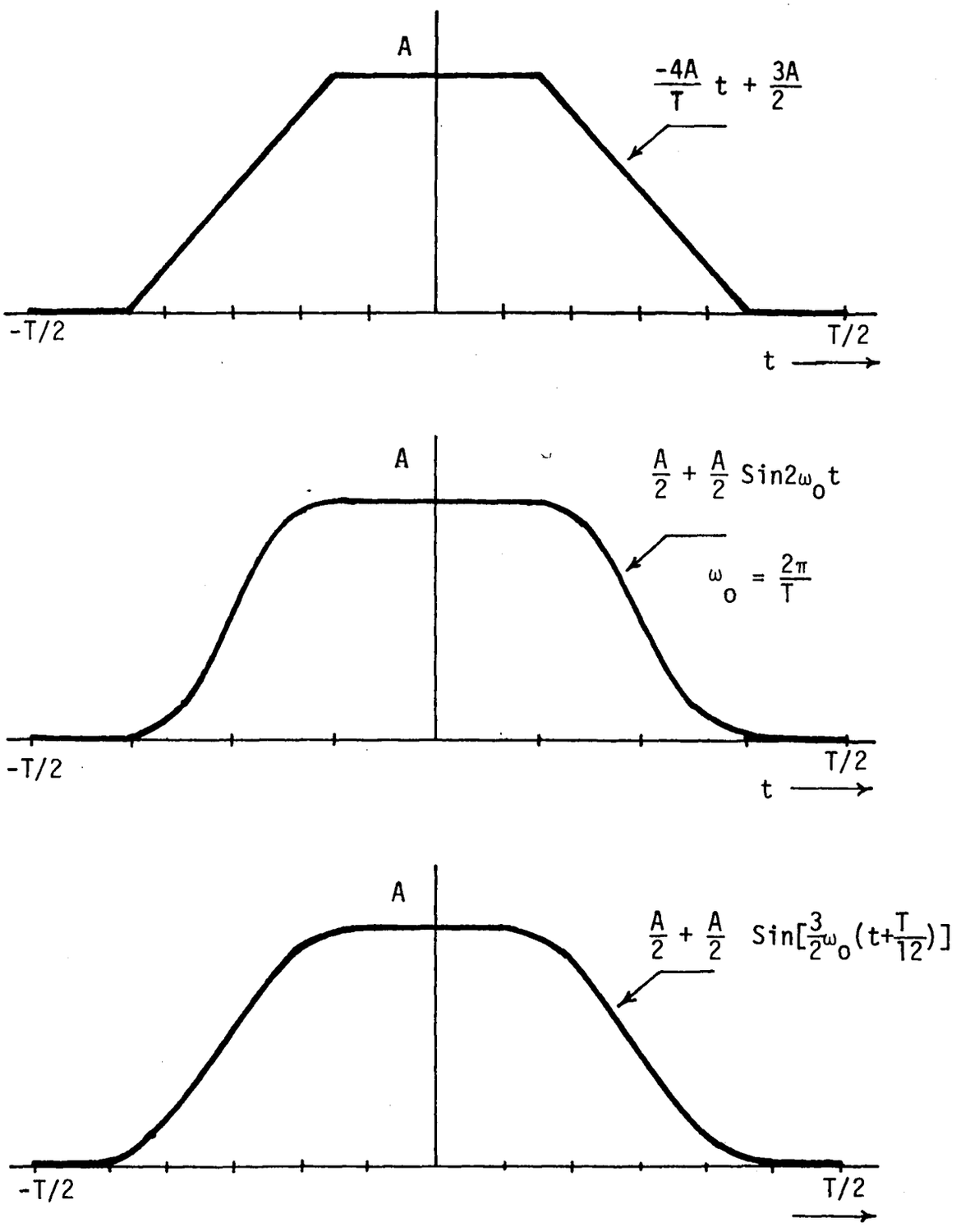

Fig. 4.3 - Pulses for telemetry

the modulating signal should be selected to produce a similar spectrum when the filters are removed.

In general, the modulating pulse train should preserve some of the flat top portion of the rectangular pulse train. This will assure good performance and will simplify implementation. Thus a compromise between the opposing requirements of flat-top pulses and narrow bandwidth must be accommodated. The broad bandwidth resulting from modulation by a rectangular pulse train is due to instantaneous switching or equivalently the infinitely sharp transition between frequencies. Therefore, an obvious means of reducing the bandwidth is to make the transition as smooth as possible while still preserving a portion of the flat-top pulse. In effect the smooth transition limits the bandwidth of the modulating signal and hence the bandwidth of the FM spectrum.

With this idea in mind, several types of transition were evaluated by using the algorithm given in Chapter 2 to determine the resulting FM spectrum. Three cases are shown in Figure 4.3. The first transition is linear, such that at least 50 percent of the flat top of the pulse is preserved. The second transition is a raised sine wave which also preserves at least 50 percent of the flat top of the pulse. If ω_0 is the fundamental fre-

quency of the pulse train, the sinusoidal transition frequency is $2\omega_0$. Finally the third waveform is also a raised sine wave, but only 33 percent of the flat top is preserved. In this case the frequency of the sinusoidal transition is $3/2\omega_0$. Due to the lower frequency of the transition, the spectrum of the modulating signal is further reduced over the preceding case. The resulting undesirable spectral components are significantly reduced in the FM spectrum. As a result, this waveform appears to easily meet the telemetry specifications [9] and it is the form of the modulating signal suggested for implementation.

Though the hueustic approach explained leads to a sinusoidal transition having satisfactory spectral characteristics, an alternate approach yields additional useful information about the general type of transition having acceptable spectral characteristics. In this approach a true FSK signal is generated. It is then filtered to produce a spectrum having desired characteristics. The resulting filtered FM signal is then demodulated to obtain the equivalent modulating signal. Two cases were considered. Assuming a data rate of 1Mbps (1μsec pulse width) and a frequency separation of 1.4 MHz (0.7 MHz on each side of the carrier frequency), the resulting FSK signal was filtered using a bandpass

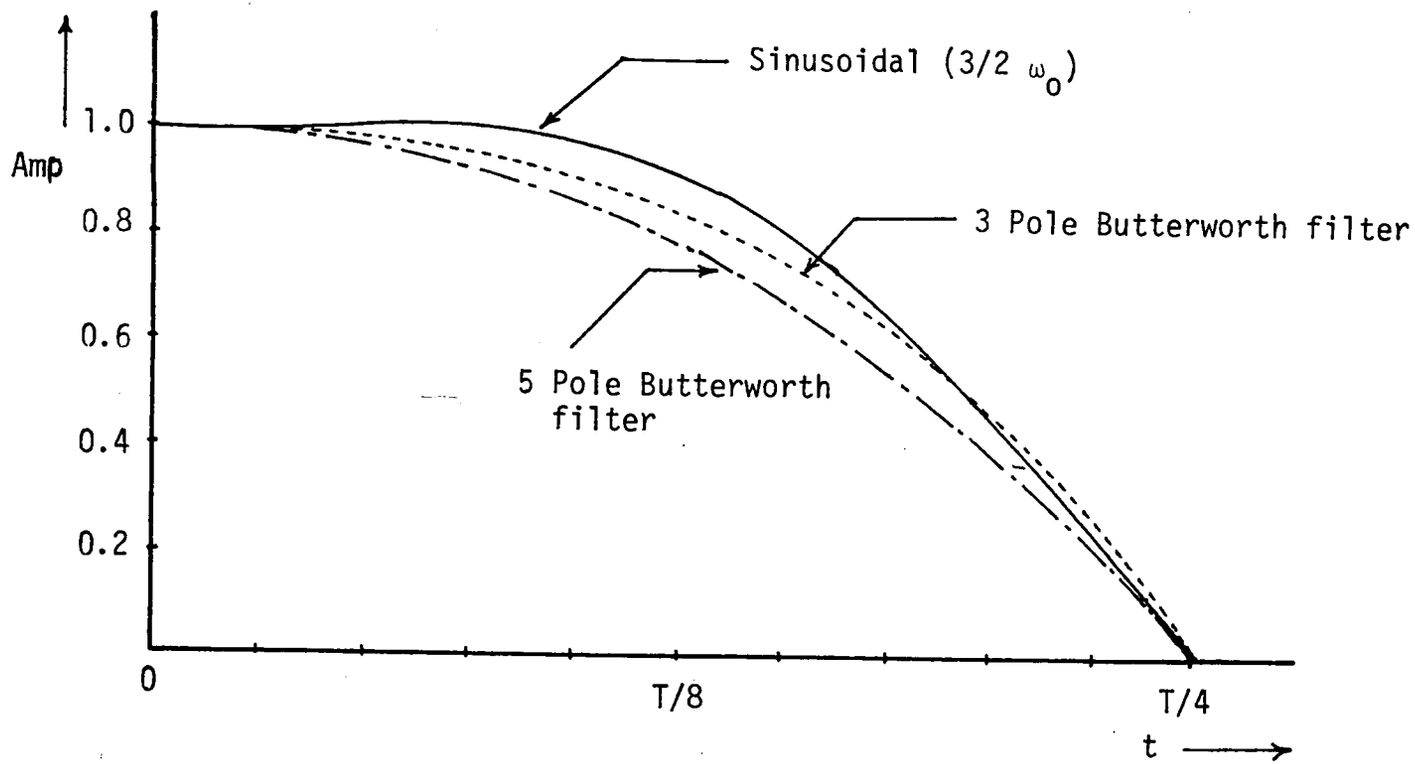

Fig. 4.4 - Comparison of the pulses for telemetry

Butterworth filter. The filter cutoff was set at ±1.2 MHz on each side of the carrier frequency. Two different filters were used, a 3-pole and a 5-pole each having the same cutoff frequencies. The resulting filtered spectrums were demodulated and the demodulated signals have been plotted in Figure 4.4 against the best sinusoidal transition determined before.

The 5-pole Butterworth filter suppresses the spectrum more than does the sinusoidal transition, but the 3-pole filter suppresses it less. All three signals meet the telemetry specifications [9], while the general shape of all three modulating signals is very similar, the sinusoidal transition produces the flattest top and is the easiest to implement. Due to the similarity between the demodulated filtered signals and the sinusoidal transition signal, the filter approach supports the hueustic selection of the sinusoidal signal obtained earlier.

4.3 Analysis

The narrow band digital FM system developed by Salz, as mentioned in Chapter 3, is claimed to be optimum, but it still lacks some practicality. The transmitting and the receiving filters, which help in reducing the overall bandwidth of the system, produce a fluctuating

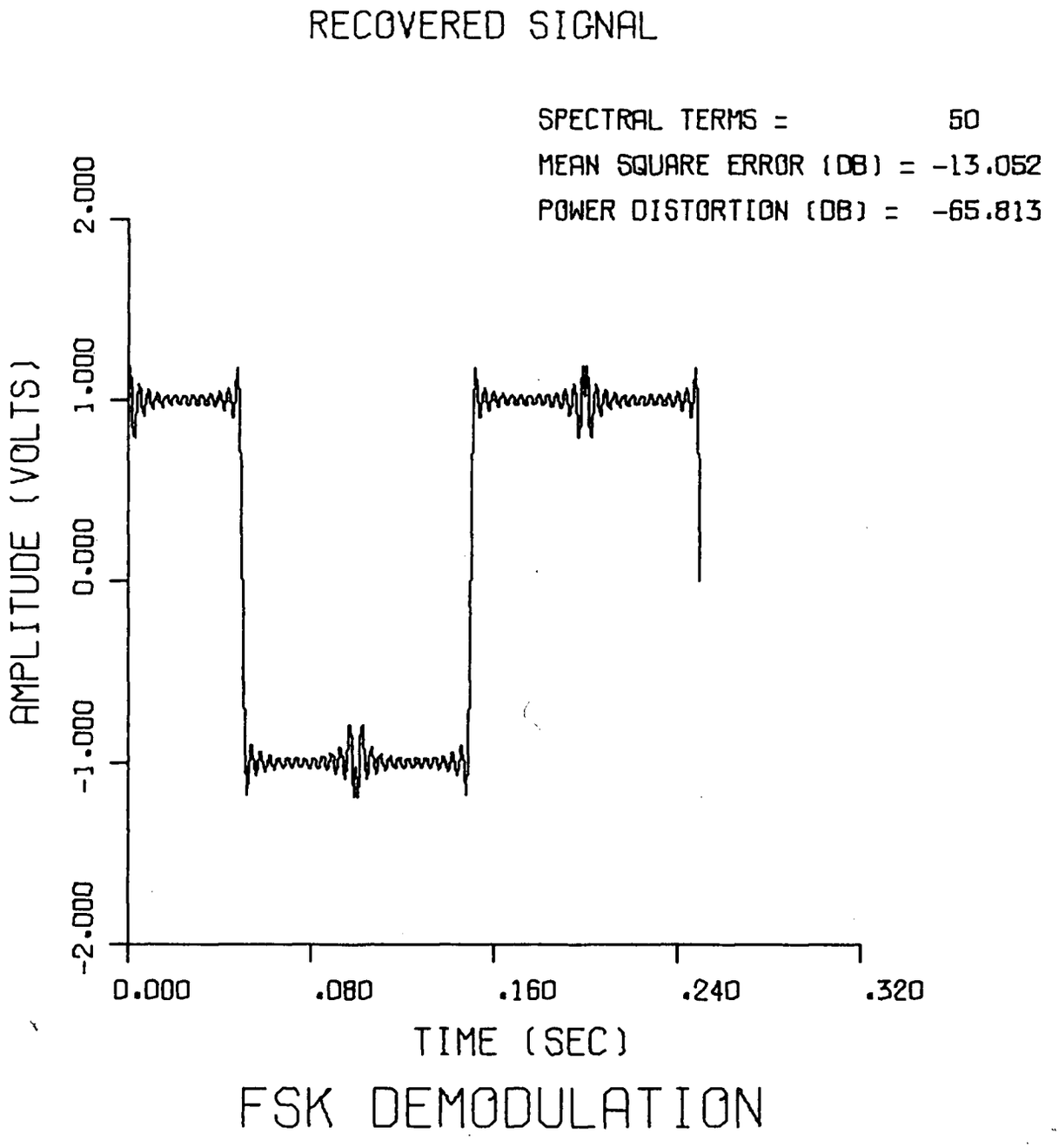

Fig. 4.5 - Signal recovered from Binary FSK spectrum

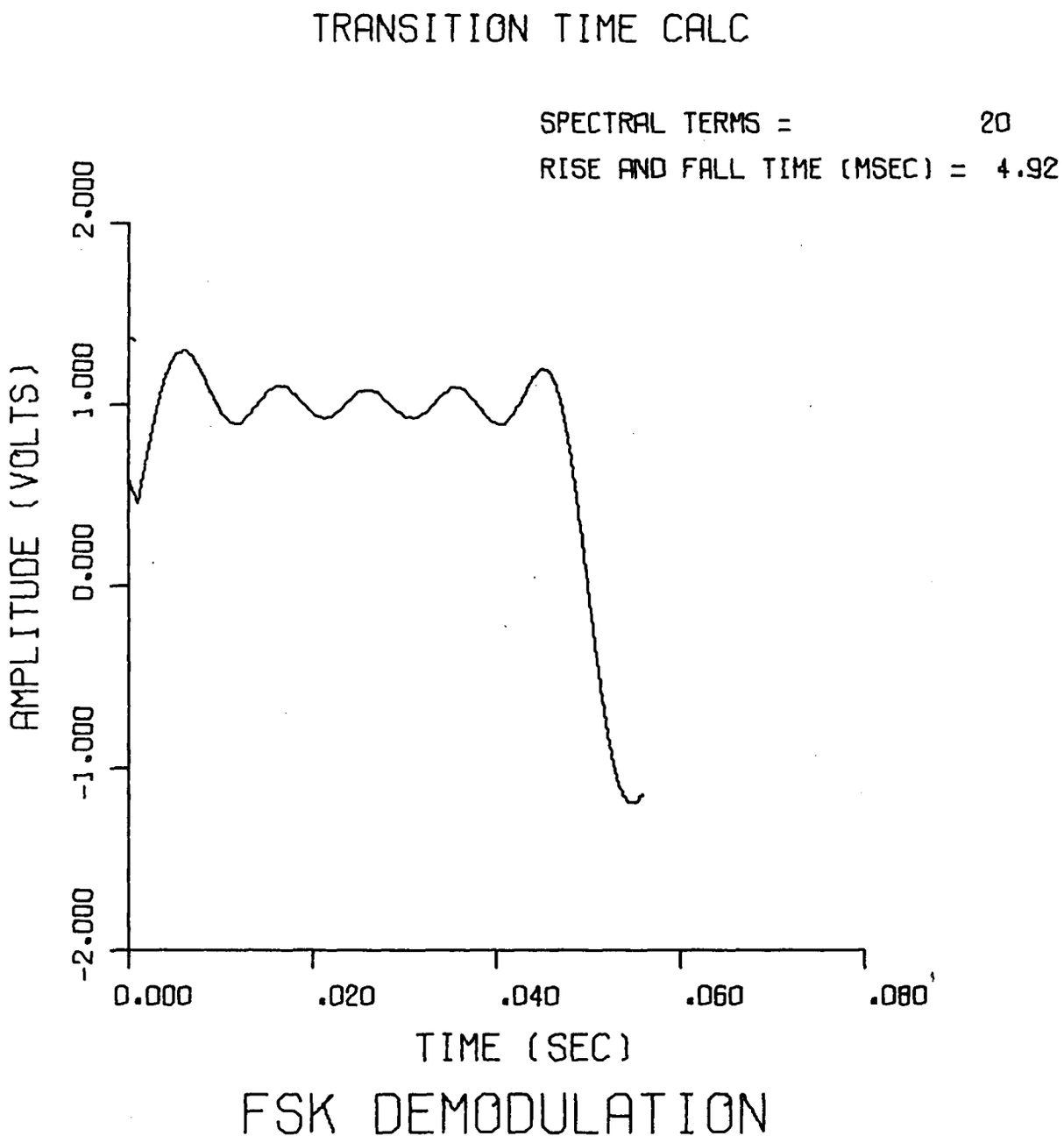

Fig. 4.6 - Calculation of the pulse transition time

envelope caused by simultaneous amplitude and frequency modulation. However, it may be difficult to realize such filters which produce an overall flat characteristic in a certain frequency range while suppressing the spectral components outside that range. An assumption is made that by selecting $\Delta\omega = \pi/LT$, the sidebands beyond $3\pi/2T$ radians per second can be neglected because they are very small in magnitude. However, this may introduce distortion in the recovered signal (time domain) and hence affect the decision threshold.

Spectrum of the binary FSK signal having a peak to peak frequency deviation equal to 50 percent of the bit rate as suggested by Salz is obtained by using the algorithm discussed in Chapter 2. Recovery of the transmitted signal from the spectrum is done by simulating the demodulation scheme outlined in this chapter. Figure 4.5 shows a received signal recovered from the FSK spectrum. A data pulse, recovered by using only twenty spectral terms from the FSK signal spectrum, and its rise time is given in Figure 4.6. A plot has been drawn in Figure 4.7 between the power in the suppressed sidebands and the number of sidebands considered. It can be seen from this plot that most of the power of an FSK signal is concentrated in the sidebands lying in the vicinity of the carrier, as claimed by Salz in his work.

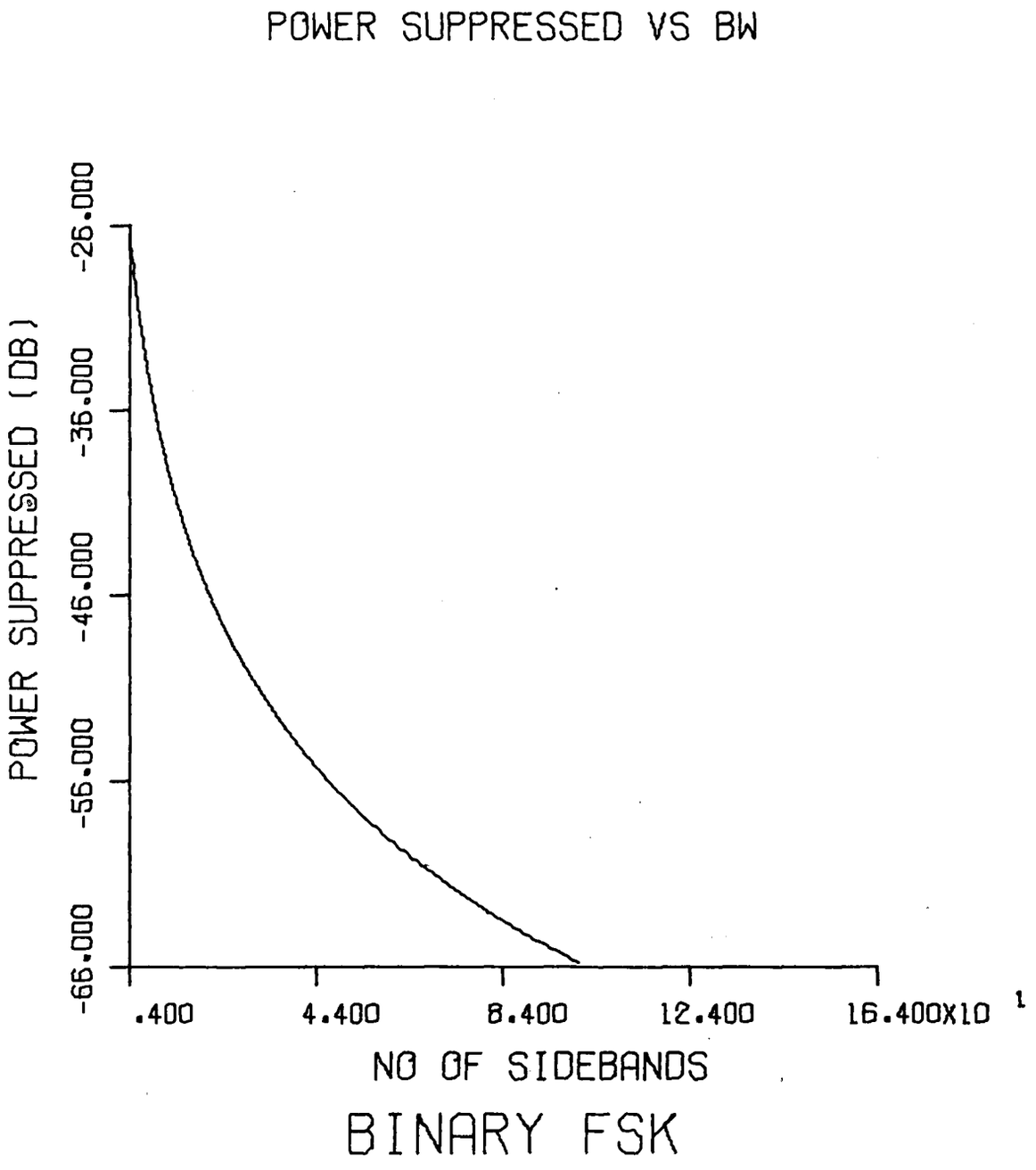

Fig. 4.7 - Plot of the power in the suppressed sidebands versus the number of sidebands

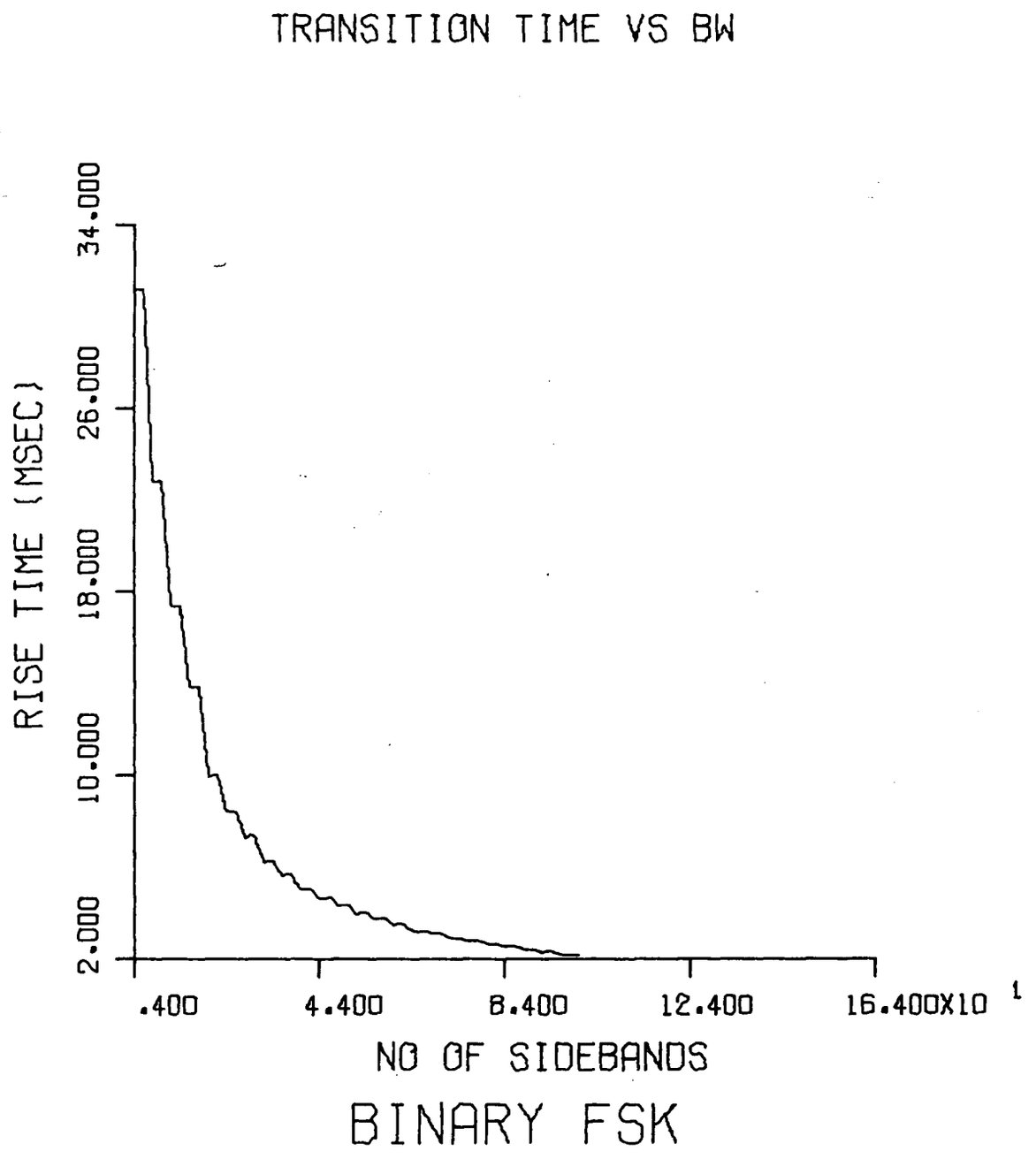

Fig. 4.8 - Plot of the rise time versus the number of sidebands

The effect of restricting the bandwidth of the FSK signal on the rise time of the received data pulse is shown by the plot in Figure 4.8. The rise time decreases expotentially with the number of spectral terms considered in recovering the modulating signal from the FSK spectrum. An important effect of reduction in the bandwidth of an FSK signal ignored by Salz is the distortion in the shape of the received data pulse. It is noticed that the amount of ripple in the received data pulse increases with the increase in the number of the suppressed sidebands. The received pulse is compared with the transmitted pulse and a plot between the mean-square-error and the number of sidebands considered is given in Figure 4.9. It can be observed that the mean-square-error is quite large if the number of spectral terms, accommodated to recover the modulating signal, is small.

Figure 4.10 gives a plot of the mean-square-error versus the power in the suppressed sidebands. It is obvious from the plot that the mean-square-error of the received pulse is large if the power in the suppressed sidebands is also large. Their relationship on the log-log scale is almost linear. Conclusion drawn from this analysis of binary FSK is given in the next chapter.

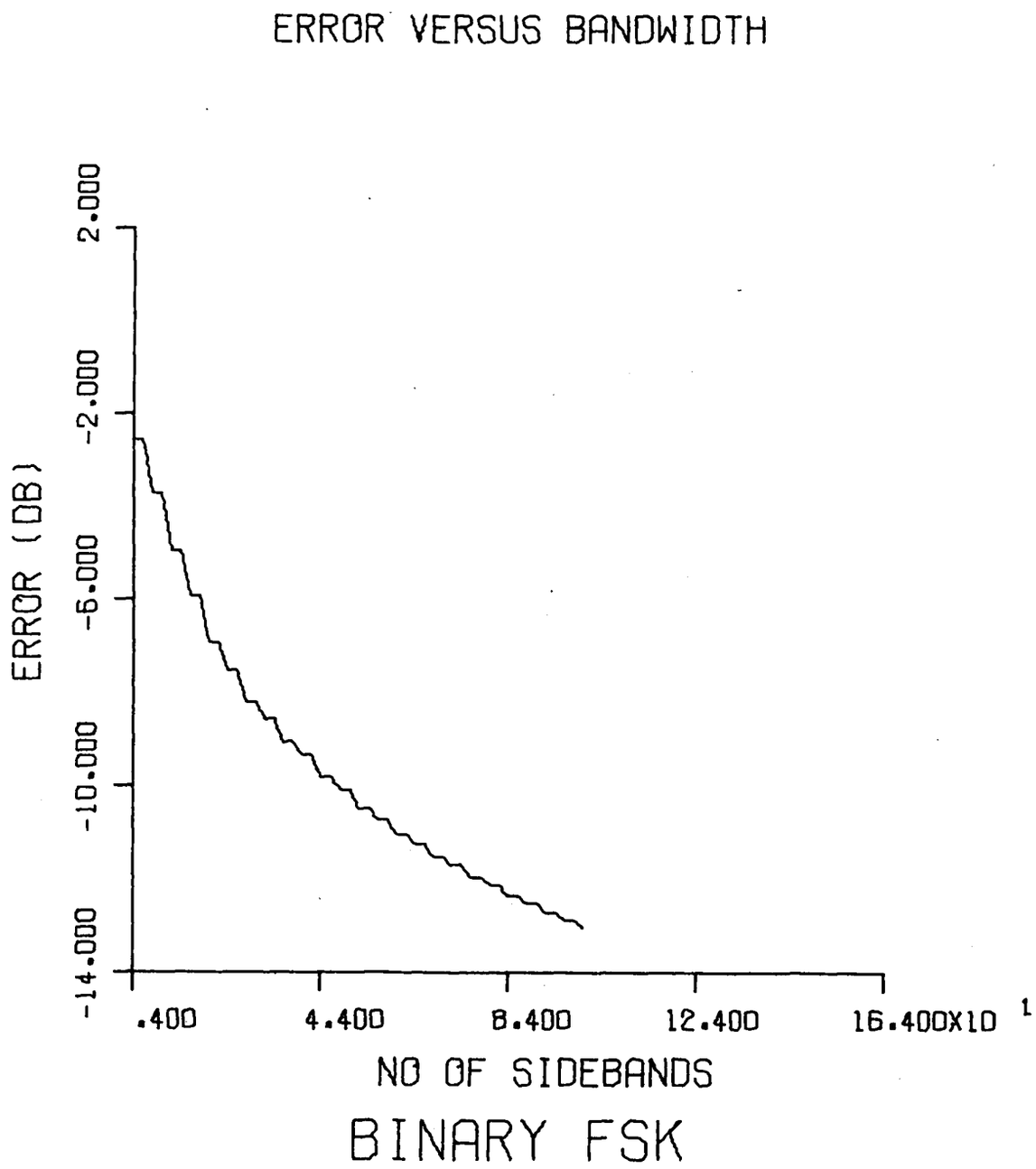

Fig. 4.9 - Plot of the mean-square-error versus the number of sidebands

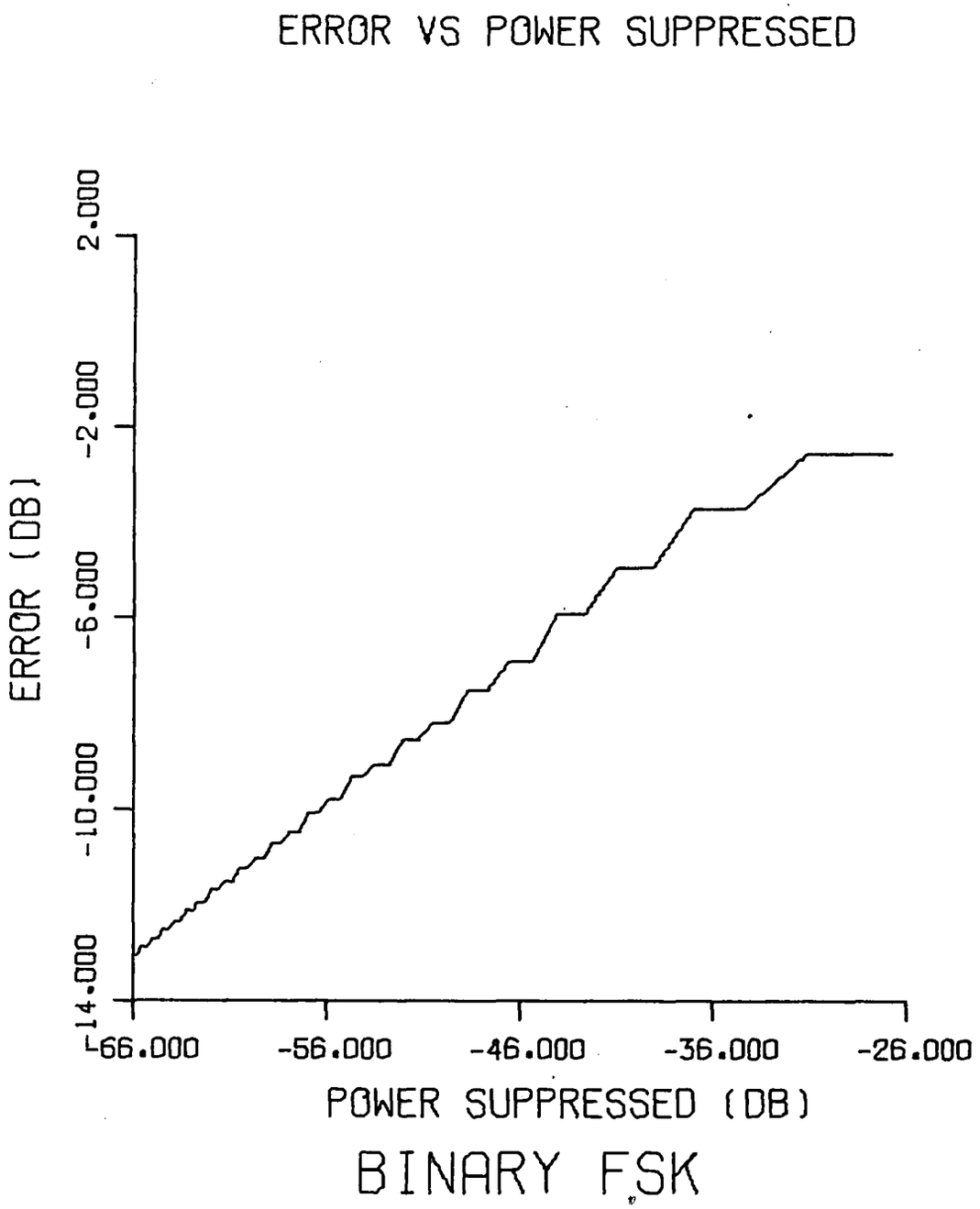

Fig. 4.10 - Plot of the mean-square-error versus the power in the suppressed sidebands

CHAPTER 5

RESULTS AND CONCLUSIONS

5.0 Introduction

In this chapter, the results of the various computer simulations regarding digital frequency modulation are discussed. A summary of the research is also provided.

5.1 Simulation Results

A binary frequency shift keying system was simulated on the digital computer using an algorithm discussed in Chapter 3. The algorithm given in Chapter 2 was also simultaneously used to find the spectrum of this system. The modulating signal for the carrier is a bi-polar square wave and therefore the instantaneous frequency may take on only two possible values. The transmitted data may be random in nature. However, the power density spectrum of a random bi-polar signal is the same as that of a square wave except that it is a continuous function of frequency, whereas, for a square wave it is discrete. Assuming a square wave as the input data, does not significantly restrict the analysis, since sufficient information regarding the bandwidth and the power of the sidebands may still be obtained for the purpose of the research. The algorithm used to find the spectrum of the binary FSK signal accepts a square wave, approximated by

four of its most significant Fourier series terms, as the modulating signal. Although the algorithm can accommodate up to eight Fourier series terms for a better approximation of a square wave, but that may require as a result, significant computation time in computing the spectrum.

Once the spectrum is obtained by using either method, the modulating signal is recovered using the demodulation algorithm. Effects of truncating or filtering the spectrum on the transmitted data train can be observed in the time domain. The mean-square-error in the recovered signal and the power in the sidebands suppressed by filtering the spectrum is correlated. The variation in the rise and the fall time of the data pulses caused by restricting the bandwidth of the system is observed and plotted.

If the simulation is carried out according to the specifications suggested by Salz, it is observed that most of the power as pointed out by Salz is concentrated within a narrow band of frequencies around the carrier. But if elimination of the sidebands outside the range

$$\omega_c - 3\pi/2T \leq \omega \leq \omega_c + 3\pi 2T$$

is done according to his analysis, distortion in the shape and perturbations in the amplitude of the recovered data pulses is observed. This may effect the decision

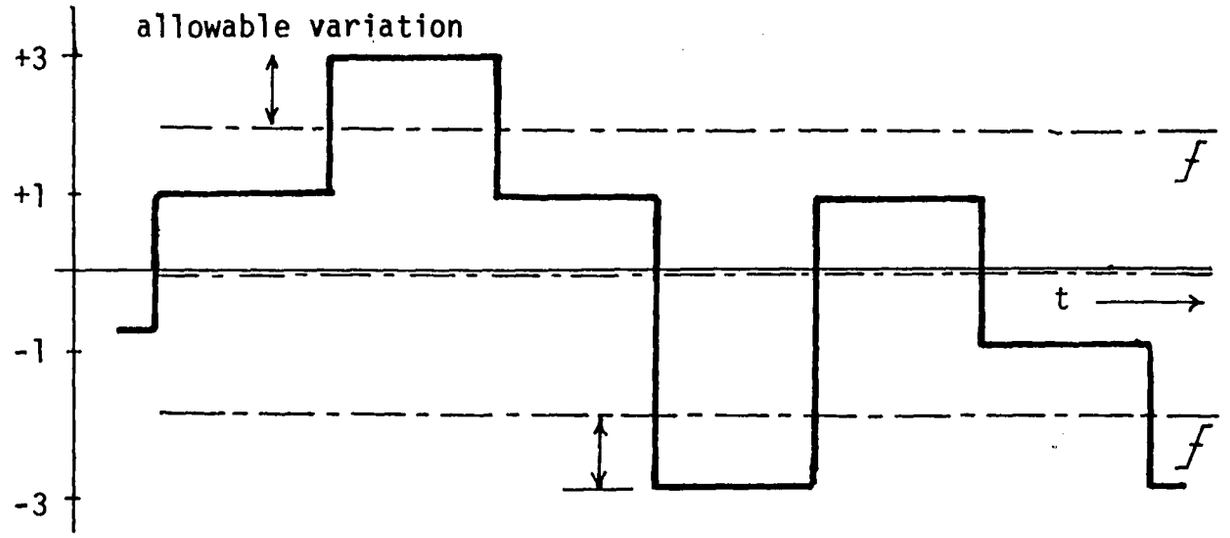

Fig. 5.1(a) - Data recovered from a broad band FSK signal

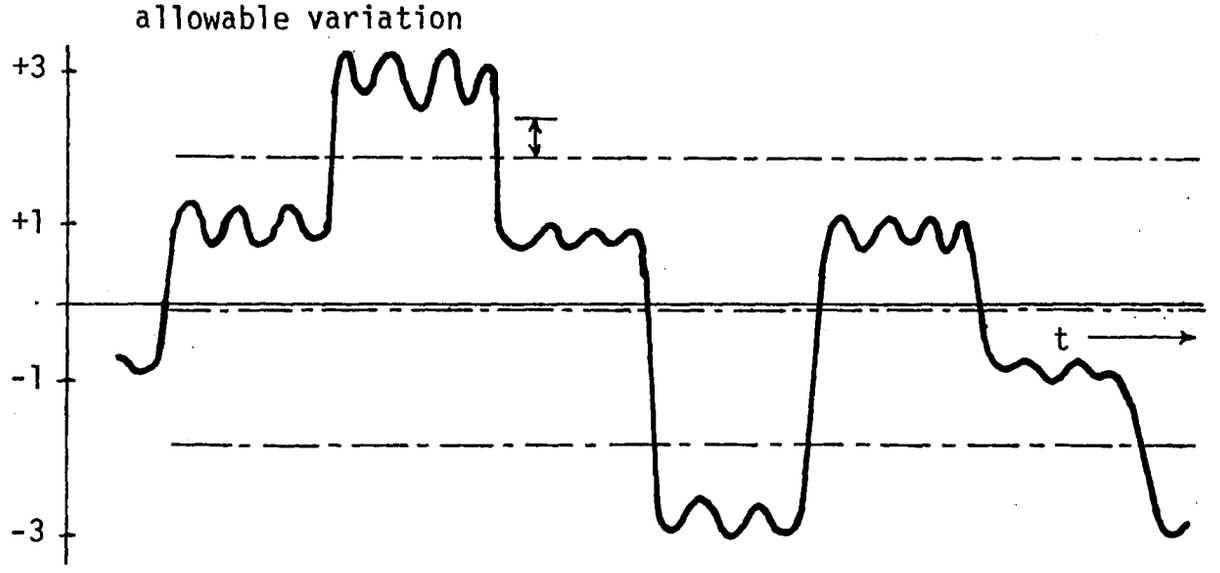

Fig. 5.1(b) - Data recovered from an FSK signal having restricted bandwidth

process particularly when multi-level pulses are transmitted as shown in Figure 5.1.

5.2 Summary and Conclusions

In this thesis a computer program has been developed which simulates any frequency modulated system. The simulation includes the generation of an FM signal for any modulating signal, determination of the spectrum of this signal, and recovery of the modulating signal from the spectrum. Analysis of an FSK system using pulse shaping for telemetry purposes is included as an application of this computer simulation. The accuracy of the computed spectrum increases with the number of the Fourier series terms used to approximate the modulating signal, but at the cost of large computation time.

The algorithm for the limiter-discriminator demodulation recovers the transmitted signal from the narrow band FM signal with great accuracy. However, if the frequency deviation is very large, it requires an increase in the number of the sample points to be taken to observe large changes in the frequency of the carrier in a short time. This may require large computer memory and computation time. If the sidebands that lie outside the frequency range as specified by Salz are suppressed completely, the distortion in the pulse shape and the

amplitude is large. This may cause the probability of error to be larger than indicated by Salz. The ripples in the received signal may be reduced by keeping the overall amplitude characteristic of the transmitting and the receiving filters flat in the range

$$\omega_c - 3\pi/2T \leq \omega \leq \omega_c + 3\pi/2T$$

and allowing a gradual roll-off in the transition band instead of a very sharp cut-off. This may be obtained by letting these filters follow Butterworth or Gaussian roll-off. This modification in the characteristic of the filters may cause the system to loose its optimality which is an important aspect of Salz's work and enabled him to make his system comparable in performance to antipodal digital data transmission. However, the changes in the filter characteristic may give more simplicity in the design and ease in the physical realization of these filters.

A plot between the mean-square-error and the power in the suppressed sidebands has been obtained. Also, the effect on the transition time of the transmitted pulse by restricting the bandwidth of the FSK signal has been observed which may help in designing the bandwidth requirements or pulse shaping of an FSK system.

REFERENCES

[1] Bennet, W. R. and Davey, J. R., "Data Transmission" pp 165-190, McGraw Hill Book Company, 1965.

[2] Kotelnikov, V. A., "The Theory of Optimum Noise Immunity", Sect. 4.9, pp 39-42, McGraw Hill Book Company, New York, 1960.

[3] Lam, Harry Y. F., "Analog and Digital Filter-Design and Realization", pp 225-240, Prentice-Hall Series, 1979.

[4] Lucky, R. W., Salz, J. and Weldon, E. J., Principles of Data Communication", pp 200-232, McGraw Hill Book Company, 1968.

[5] Panter, P. F., "Modulation, Noise and Spectral Analysis", pp 254-266, 406-410, McGraw Hill Book Company, 1965.

[6] Salz, J., "Performance of Multilevel Narrow Band FM Digital Communication Systems", IEEE Trans on Communication Technology, Vol. COM-13, Dec, 1965.

[7] Salz, J., "The Spectral Density Function of Multi-Level Continuous Phase FM", IEEE Trans on Information Theory, Vol. IT-11, pp 429-433, July, 1965.

[8] Stearns, S. D., "Digital Signal Analysis", Hayden Book Company, Inc., New Jersey, 1975.

[9] IRIG Standard, 106-77, Telemetry Standards, Telemetry Group, Inter-range Instrumentation Group, Range Commanders Council, Pub. Secretariat Range Commanders Council, New Mexico, Nov., 1977.

APPENDIX A

SIMULATION OF A FREQUENCY MODULATED SYSTEM

A flow chart of the computer program used to simulate a frequency modulation system is given in this appendix. The flow chart notation confirms with the IBM specifications, however, some changes are made to have compactness. Lehigh University computer CDC 6600 was used for this program. Fortran IV is the language used for the simulation.

Information regarding maximum frequency deviation (MDEV), amplitude of the modulating signal (AMP) and the number of sine and cosine terms used to approximate the modulating signal is read. BETAC, BETAS and BETA are the arrays of the modulation indices calculated by reading the spectral terms of the modulating signal. Bessel coefficients are obtained as complex arrays R, RC, RS depending whether the sine terms or the cosine terms are present.

In order to find the frequency of the sidebands, a group of eight nested subroutines is used. The frequencies of the upper and the lower sidebands are given by the arrays UPSB and LOSB, whereas the amplitudes are given by the arrays SBU and SBL respectively. The power in the suppressed sidebands can be obtained from the

array DIST. Many figures have been included in this appendix which explain the logic of this simulation.

```
DIMENSION BETA(L), SC(L,N)
SS(L,N), R(L,N), SBU(M),
SBL(N), IFREQ(L), IUPSB(N),
LOSB(N)
COMMON |ABDUL|
COMMON |RABIA|
COMPLEX R, RC, RS, SBU, SBL, CARIR
REAL MDEV, IFREQ, IUPSB, LOSB
DATA M
```

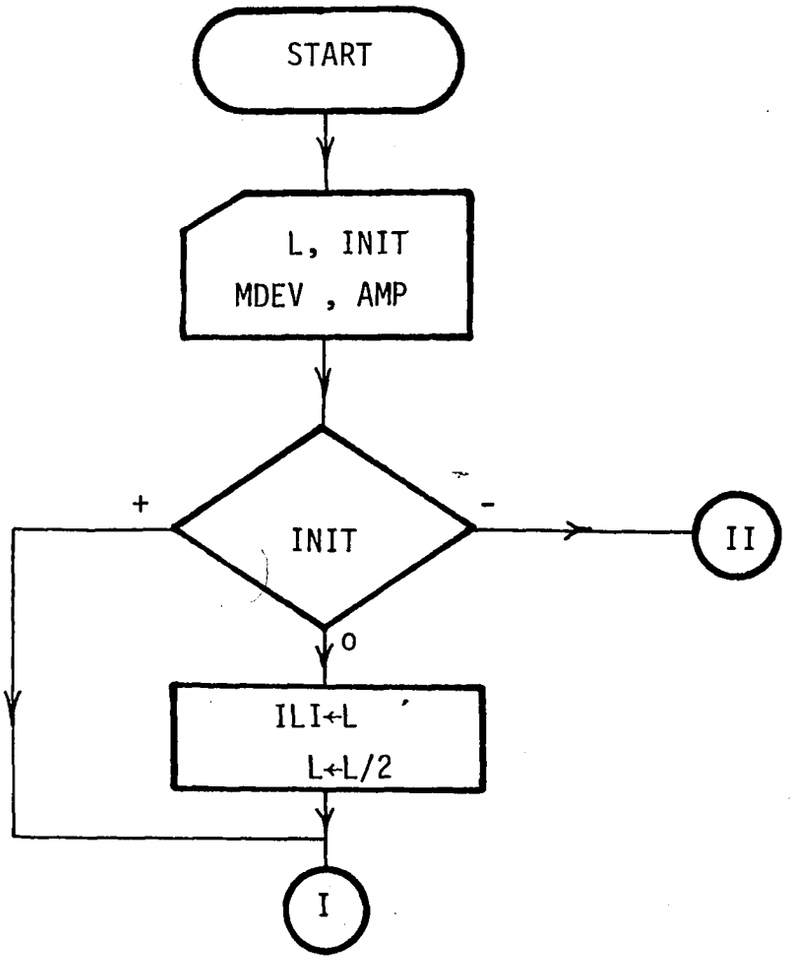

Fig. A.1 - Initialization of the main program

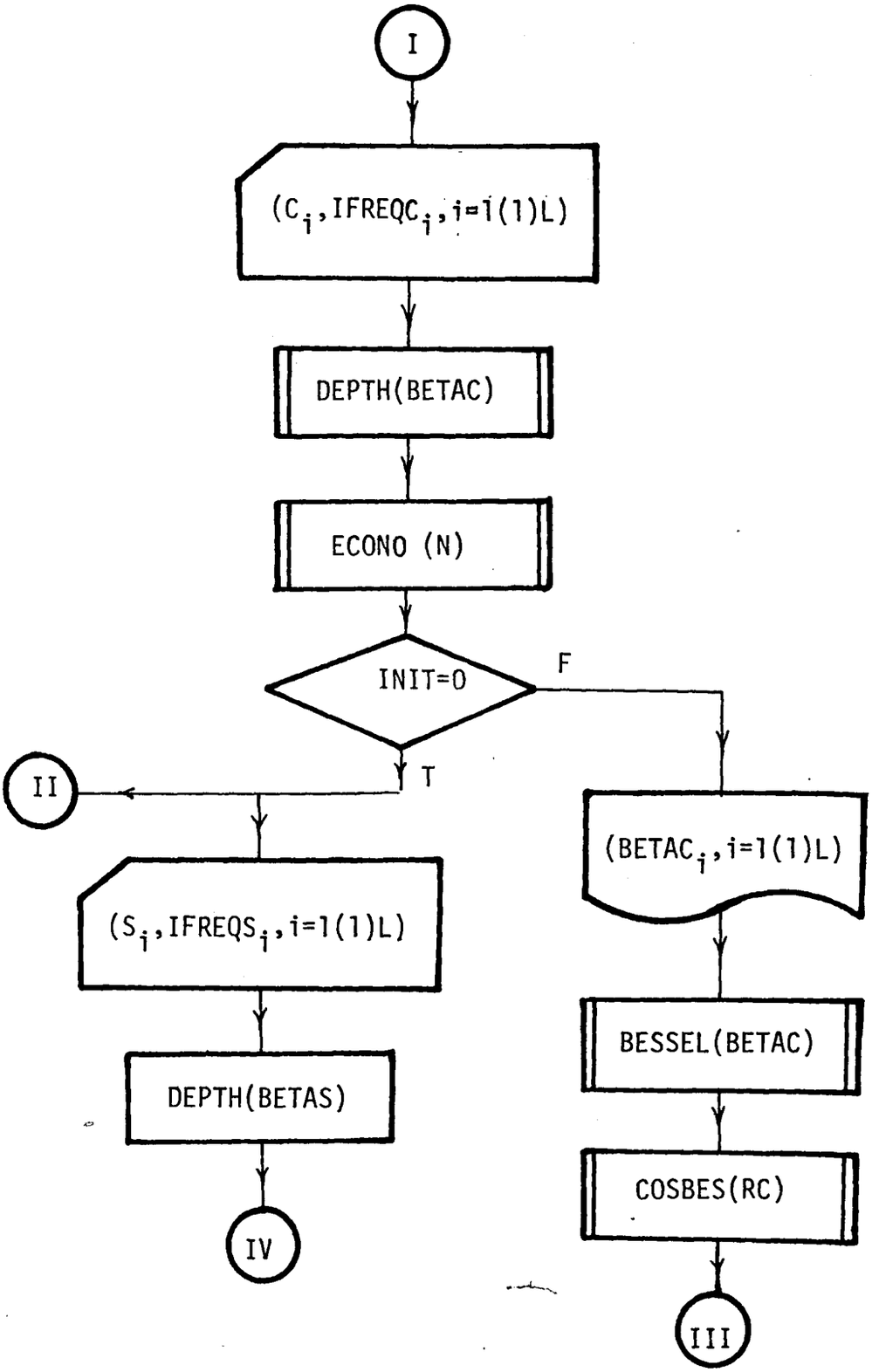

Fig. A.2 - Calculation of the Modulation Indices

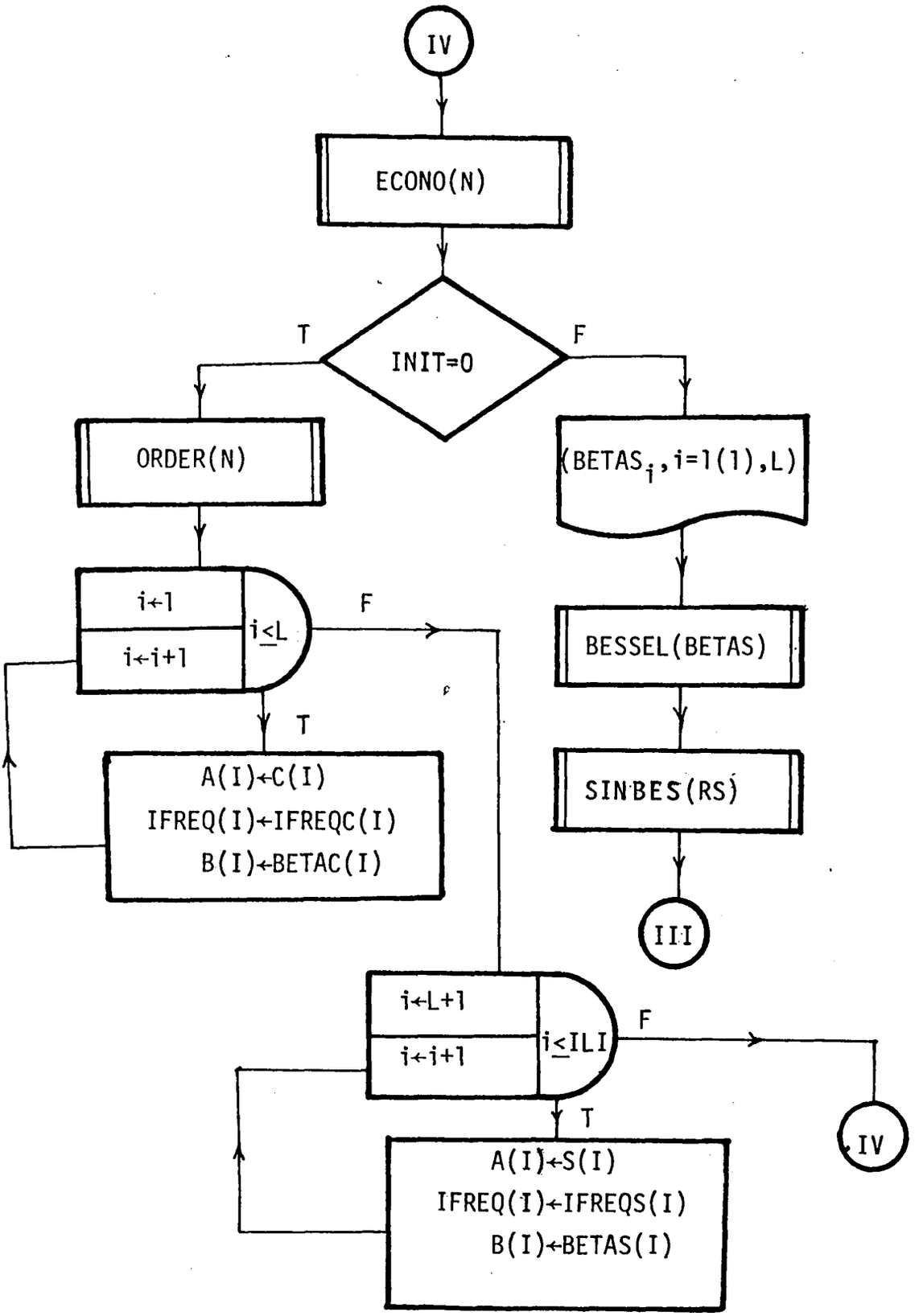

Fig. A.3 - Calculation of the Bessel coefficients

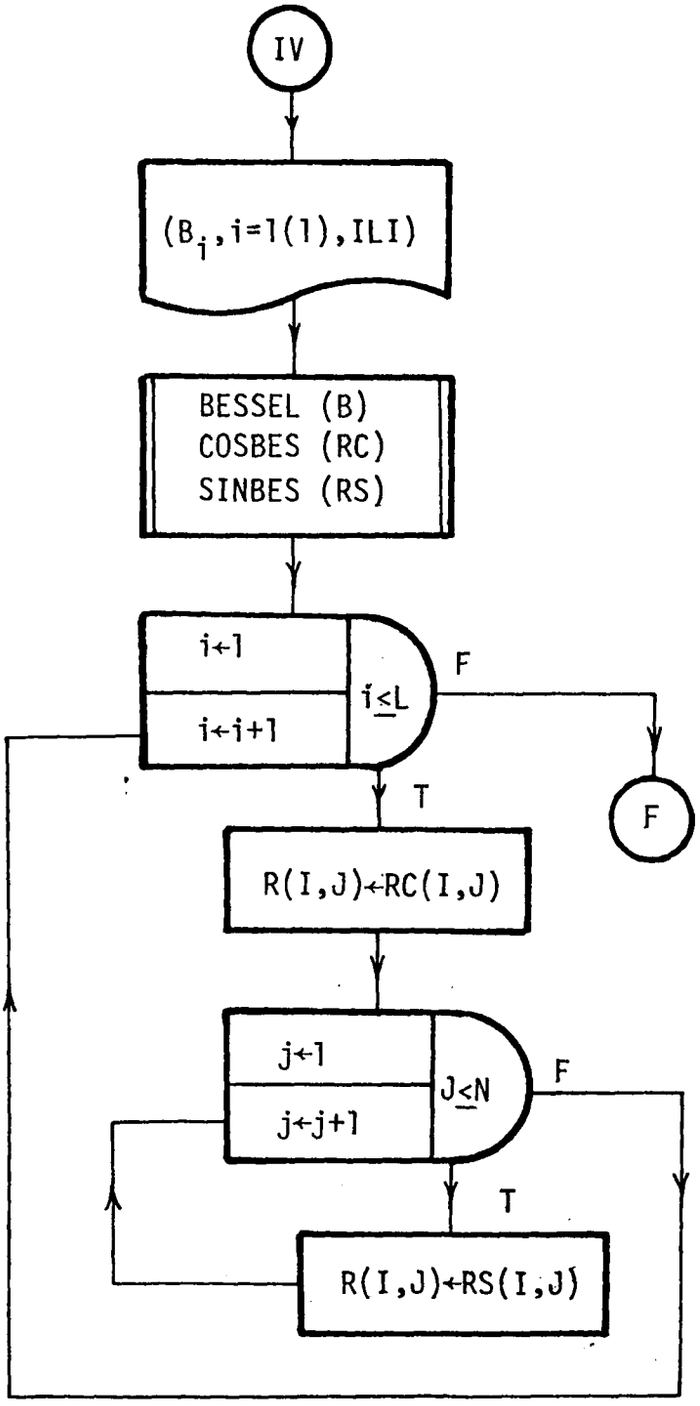

Fig. A.4 - Combination of the Bessel coefficients

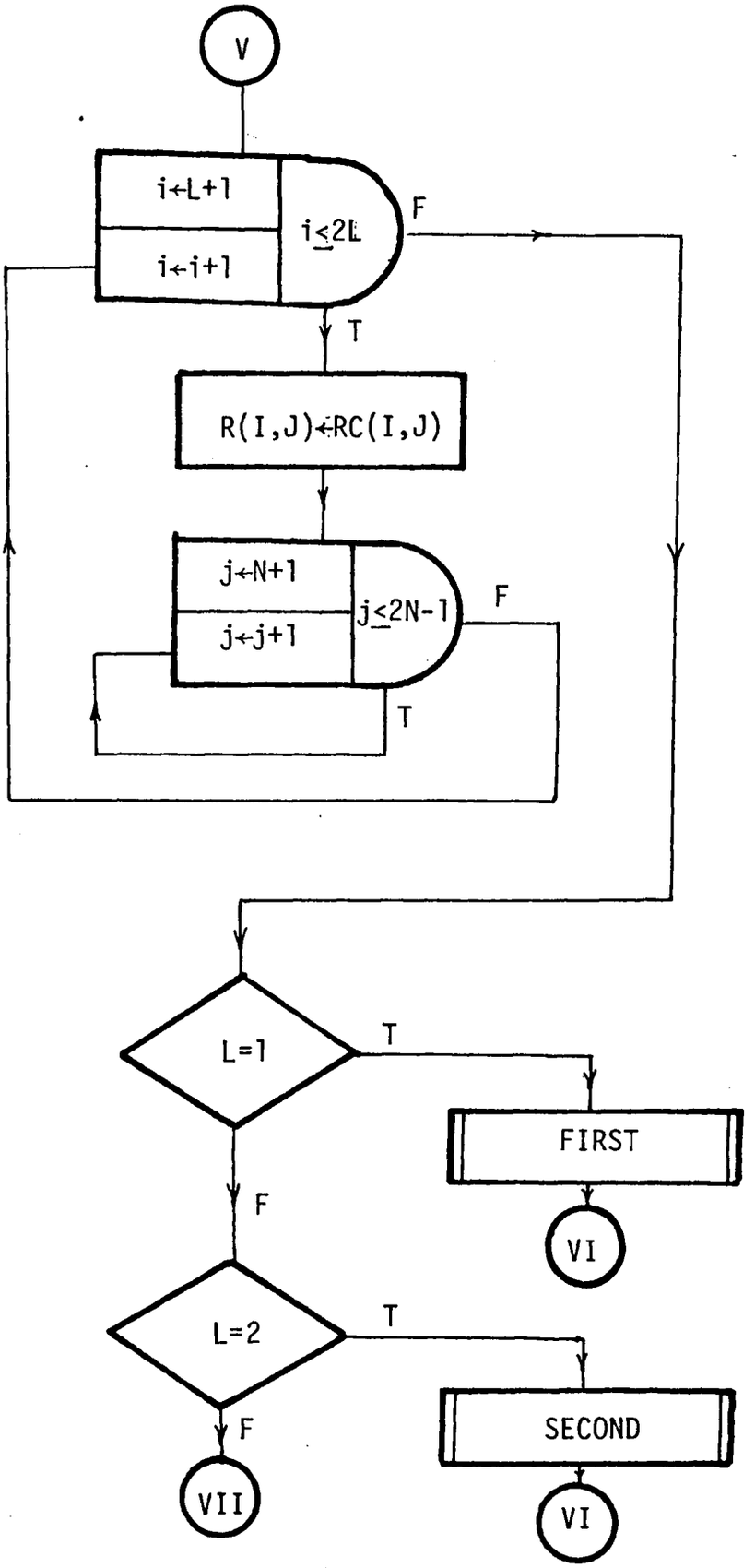

Fig. A.5 - Calculation of the sideband frequencies

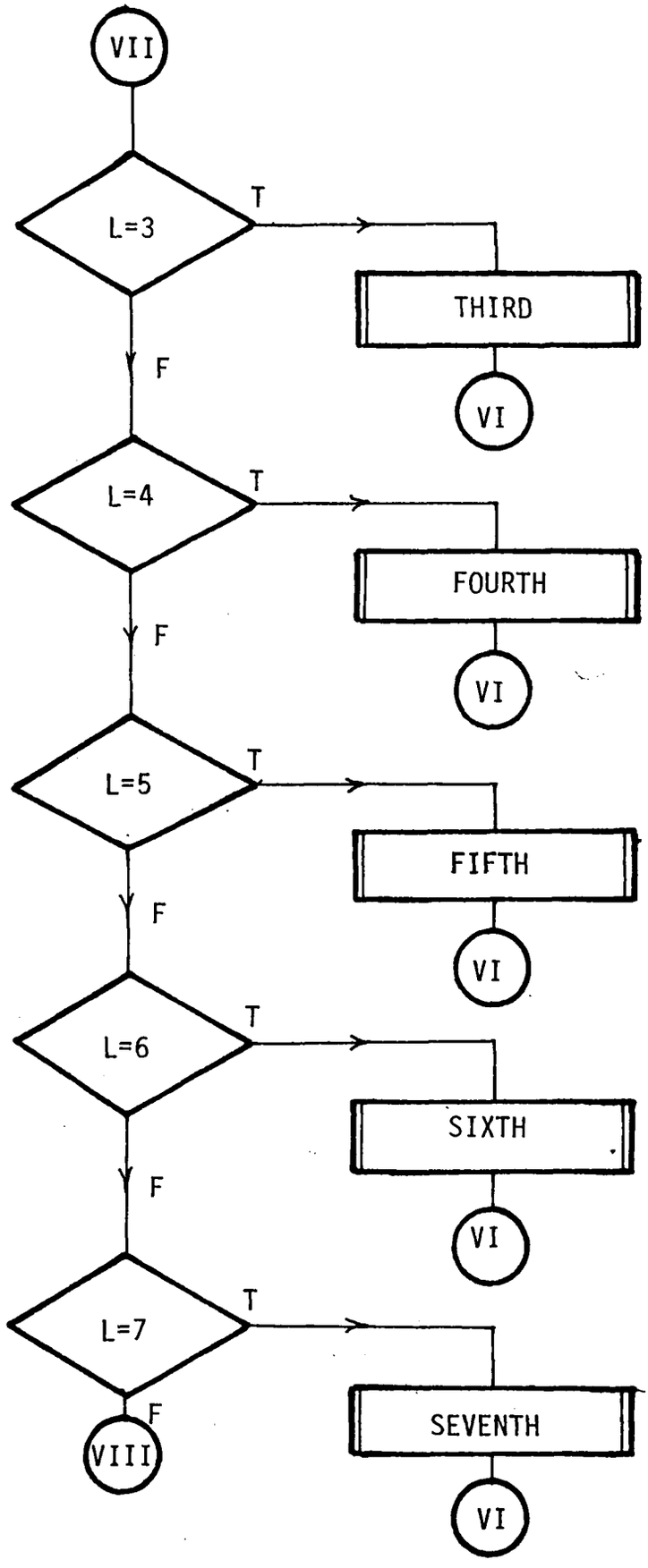

Fig. A.6 - Calculation of the sideband frequencies

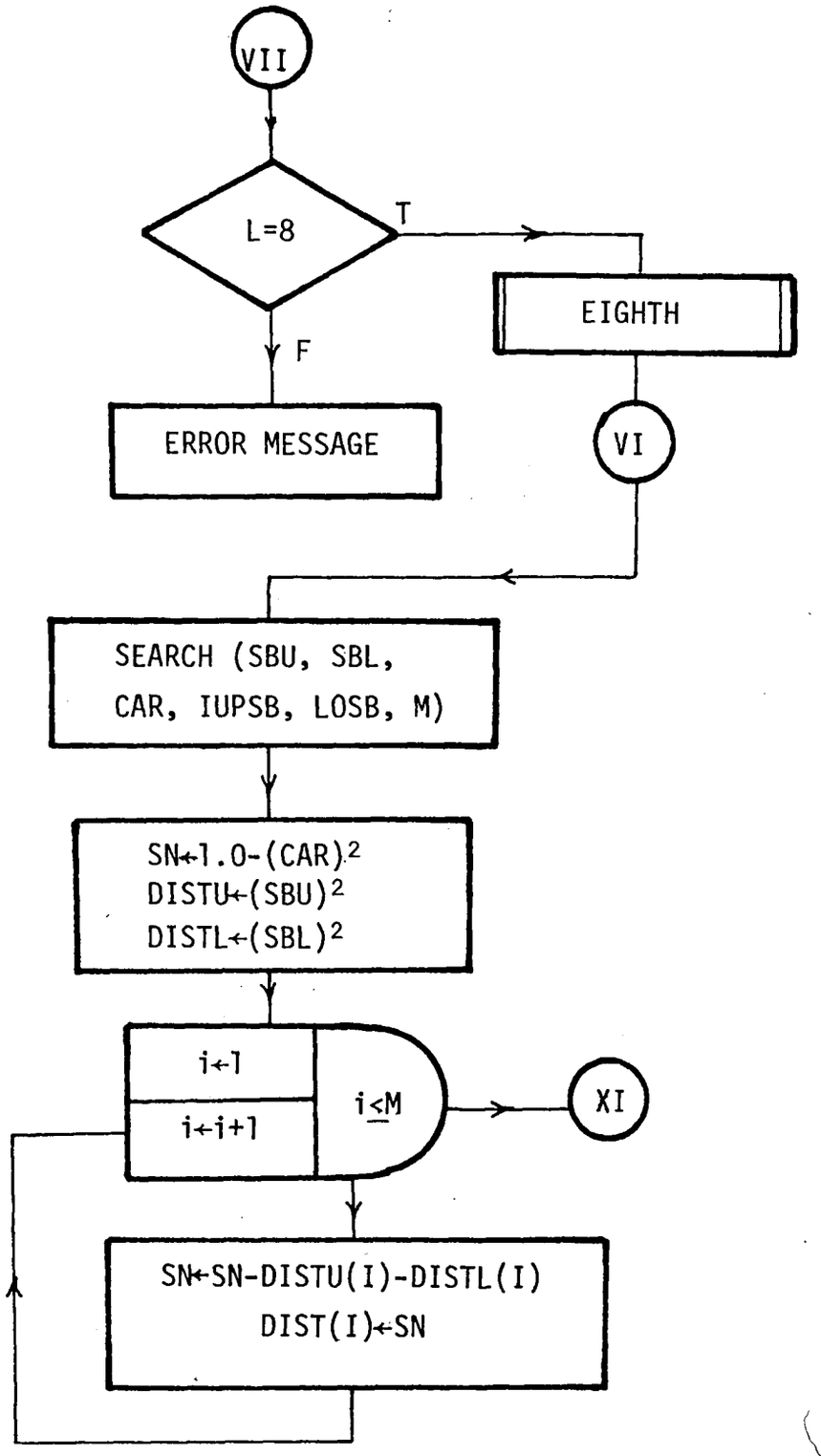

Fig. A.7 - Calculation of the amplitude of the Sidebands and the power suppressed

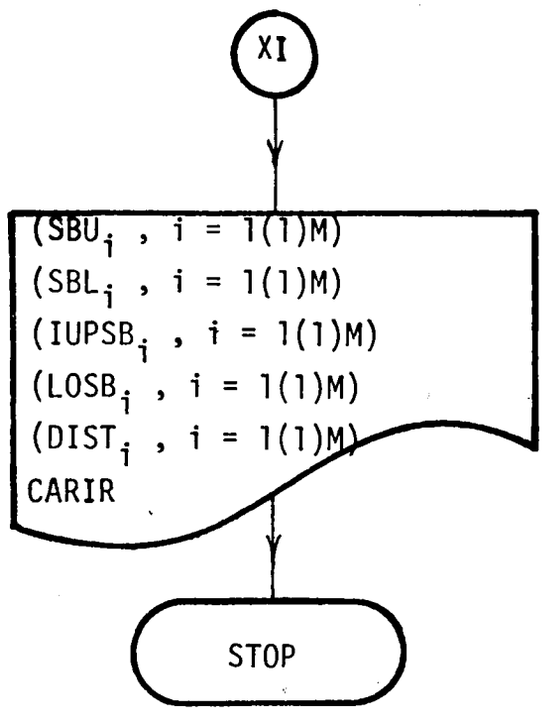

Figure A.8 - Printing of the results

VITA

Arif Kareem, son of Rabia and Abdul, was born in Lahore, Pakistan on February 3, 1953. He obtained his high school education from the local institutions. He received his Bachelor of Science in Electrical Engineering from the University of Engineering and Technology, Lahore, Pakistan in 1975. He came to the United States in 1978 and was a Teaching Assistant at Lehigh University, Bethlehem, Pennsylvania from 1978 to 1980 where he completed requirements for his Master of Science degree in Electrical Engineering.